

## Discovery of Tricyclic Indoles That Potently Inhibit Mcl-1 Using Fragment-Based Methods and Structure-Based Design

Jason P. Burke, zhiguo bian, Subrata Shaw, Bin Zhao, Craig M. Goodwin, Johannes Belmar, Carrie F. Browning, Dominico Vigil, Anders Friberg, DeMarco Camper, Olivia W. Rossanese, Taekyu Lee, Edward T Olejniczak, and Stephen W. Fesik

*J. Med. Chem.*, **Just Accepted Manuscript** • Publication Date (Web): 06 Apr 2015

Downloaded from <http://pubs.acs.org> on April 7, 2015

### Just Accepted

"Just Accepted" manuscripts have been peer-reviewed and accepted for publication. They are posted online prior to technical editing, formatting for publication and author proofing. The American Chemical Society provides "Just Accepted" as a free service to the research community to expedite the dissemination of scientific material as soon as possible after acceptance. "Just Accepted" manuscripts appear in full in PDF format accompanied by an HTML abstract. "Just Accepted" manuscripts have been fully peer reviewed, but should not be considered the official version of record. They are accessible to all readers and citable by the Digital Object Identifier (DOI®). "Just Accepted" is an optional service offered to authors. Therefore, the "Just Accepted" Web site may not include all articles that will be published in the journal. After a manuscript is technically edited and formatted, it will be removed from the "Just Accepted" Web site and published as an ASAP article. Note that technical editing may introduce minor changes to the manuscript text and/or graphics which could affect content, and all legal disclaimers and ethical guidelines that apply to the journal pertain. ACS cannot be held responsible for errors or consequences arising from the use of information contained in these "Just Accepted" manuscripts.



**ACS Publications**  
High quality. High impact.

# Discovery of Tricyclic Indoles That Potently Inhibit Mcl-1 Using Fragment-Based Methods and Structure-Based Design

*Jason P. Burke<sup>+</sup>, Zhiguo Bian, Subrata Shaw, Bin Zhao, Craig M. Goodwin, Johannes Belmar, Carrie F. Browning, Dominico Vigil<sup>#</sup>, Anders Friberg<sup>^</sup>, DeMarco V. Camper, Olivia W. Rossanese, Taekyu Lee, Edward T. Olejniczak, and Stephen W. Fesik\**

Department of Biochemistry, Vanderbilt University School of Medicine, 2215 Garland Avenue, 607 Light Hall, Nashville, Tennessee 37232-0146, USA

## KEYWORDS:

Fragment-based screening; apoptosis; cancer; Mcl-1; inhibitor; drug discovery

1  
2  
3 Abstract  
4

5  
6 Myeloid cell leukemia-1 (Mcl-1) is an anti-apoptotic member of the Bcl-2 family of proteins that  
7  
8 is overexpressed and amplified in many cancers. Overexpression of Mcl-1 allows cancer cells to  
9  
10 evade apoptosis and contributes to the resistance of cancer cells to be effectively treated with  
11  
12 various chemotherapies. From an NMR-based screen of a large fragment library, several distinct  
13  
14 chemical scaffolds that bind to Mcl-1 were discovered. Here, we describe the discovery of potent  
15  
16 tricyclic 2-indole carboxylic acid inhibitors that exhibit single digit nanomolar binding affinity to  
17  
18 Mcl-1 and greater than 1700-fold selectivity over Bcl-xL and greater than 100 fold selectivity  
19  
20 over Bcl-2. X-ray structures of these compounds when complexed to Mcl-1 provide detailed  
21  
22 information on how these small-molecules bind to the target, which was used to guide compound  
23  
24 optimization.  
25  
26  
27  
28  
29  
30  
31  
32  
33  
34  
35  
36  
37  
38  
39  
40  
41  
42  
43  
44  
45  
46  
47  
48  
49  
50  
51  
52  
53  
54  
55  
56  
57  
58  
59  
60

## INTRODUCTION

The intrinsic apoptosis pathway is tightly regulated by a balance of pro-apoptotic and anti-apoptotic proteins that respond to numerous extracellular and intracellular stresses, including growth factor and oxygen deprivation, DNA damage, oncogene induction, metabolic changes, and the effects of cytotoxic drugs.<sup>1</sup> In normal cells, these stresses induce oligomerization of the pro-apoptotic proteins Bax and Bak at the mitochondrial outer membrane, which triggers cytochrome c release and caspase-dependent apoptosis.<sup>2</sup> Anti-apoptotic Bcl-2 family proteins, including Bcl-2, Bcl-xL, Bcl-w, Bcl-A1, and Mcl-1, bind to and sequester pro-apoptotic members of the same family, leading to the inhibition of apoptosis.<sup>3</sup> In cancers, anti-apoptotic Bcl-2-family proteins are often upregulated causing the enhancement of cancer cell survival in otherwise stressful conditions and contributes to increased resistance to anti-cancer therapeutics.<sup>4</sup>

Amplification of the gene encoding the anti-apoptotic protein Myeloid cell leukemia-1 (Mcl-1) is one of the most common genetic aberrations in human cancers.<sup>5,6</sup> Mcl-1 overexpression is associated with high tumor grade and poor survival in lung<sup>7</sup>, breast<sup>8</sup>, prostate<sup>9</sup>, pancreatic<sup>10</sup>, ovarian<sup>11</sup>, and cervical cancers<sup>12</sup>, as well as melanoma<sup>13</sup> and leukemia<sup>14</sup>. Mcl-1 activity has also been implicated in the resistance to multiple therapies, including microtubule-targeting agents like paclitaxel and vincristine, which are widely prescribed for cancer patients.<sup>15</sup> Thus, neutralizing the function of Mcl-1 holds promise as an effective strategy to restore apoptotic signaling in cancer cells and enhance the response to currently approved chemotherapeutics. Despite this compelling rationale, no clinical therapeutic agent selectively targeting Mcl-1 is currently available.

Mcl-1 mediates its effects primarily through protein-protein interactions and is therefore considered difficult to target with small molecules.<sup>16</sup> However, small molecule inhibitors that potently bind to the related family members Bcl-2 and Bcl-xL have been discovered.<sup>17-25</sup> Among them, are the Bcl-2/Bcl-xL dual inhibitor ABT-263 and the selective Bcl-2 inhibitor ABT-199, both of which are in clinical trials.<sup>24,26,27</sup> These inhibitors were reported to bind to their target proteins with 2-3 orders of magnitude higher affinities than the best Mcl-1 inhibitors reported to date in the literature.<sup>28-32</sup>

To discover Mcl-1 inhibitors, we have previously conducted a fragment-based screen of approximately 15,000 compounds using NMR and reported on the discovery of high-affinity ( $K_i$  <100 nM) inhibitors that bind to Mcl-1 starting from two classes of hits identified in the screen.<sup>28</sup> The best inhibitor in this series was an optimized 2-indole carboxylic acid derivative **1** that binds to Mcl-1 with a  $K_i$  of 55 nM.<sup>28</sup>

Several additional structurally distinct small molecules were identified in the fragment screen with similar or higher binding affinities and/or ligand efficiency (LE). One of these series contains a tricyclic indole 2-carboxylic acid core, as found in the fragment hit **2**. Here we describe the discovery of very potent Mcl-1 inhibitors that were derived from this fragment hit. These compounds have single digit nanomolar binding affinity and high selectivity for Mcl-1 over Bcl-xL and Bcl-2. Crystal structures of this series of inhibitors when bound to Mcl-1 provide detailed information on the molecular interactions that stabilize complex formation.

## Structure of Compound 1 & 2

## RESULTS AND DISCUSSION

**Synthesis.** The general synthetic approach used for synthesizing tricyclic 2-indole carboxylic

acids derivatives is illustrated in Scheme 1 - 3. The preparation of the tricyclic analogs based on the fragment hit **2** that are listed in Table 1 is depicted in Scheme 1. The appropriate bicyclic hydrazine **10** was reacted with a selected  $\alpha$ -ketoester **11** to give the tricyclic indole-2-carboxylic acid **3-8** via Fisher indole reaction<sup>33,34</sup> followed by saponification.

### Scheme 1<sup>a</sup>

The synthetic route illustrated in Scheme 2 was developed to prepare the compounds depicted in Table 2. Using the Fischer indole condition depicted in Scheme 1, the selected hydrazine **10** was cyclized with a selected  $\alpha$ -ketoacid **12** to give a mixture of corresponding tricyclic indole diester **13a** and indole acid **13b**. Formation of the tricyclic indole diester **13a** was improved by extending the reaction time, however, the reaction suffered from a poor yield. Therefore, the indole acid **13b** in the mixture was converted to the methyl ester **13c** using TMSCHN<sub>2</sub> then both indole esters **13a** and **13c** were carried to the subsequent reaction without isolation. The alcohol **14** was prepared by selective reduction of the extended ethyl ester at the 3-position of the indole using BH<sub>3</sub>-THF. Mitsunobu condensation (as used in our previous report<sup>28</sup>) was used to couple a selected phenol to yield the phenyl ether **15**. Subsequent saponification of the ester gave the desired carboxylic acid moiety in compounds **16-21**, **23**, **26-33**. The sulfide groups in the tricyclic indole acids **19** and **23** were oxidized to the corresponding sulfoxide **24** or sulfone **22** and **25** using *m*-CPBA.

### Scheme 2<sup>a</sup>

Tricyclic 6-Cl-2-indole carboxylic acid **34** and **35** were prepared as outlined in Scheme 3. 2-Br-3-Cl-aniline **38** was converted to the indole **39** utilizing the modified Japp-Klingemann reaction condition.<sup>28</sup> Selective BH<sub>3</sub> reduction followed by a Mitsunobu reaction gave the indole

ester **41**. Alkylation at the indole nitrogen gave compound **42**, which underwent a radical cyclization to yield the tricyclic indole ester containing the piperidine C-ring. Subsequent saponification gave the desired acid **34**. The intermediate **41** was converted to the pinacol borate **43**, which was oxidized to give the phenol **44**. The morpholine C-ring was constructed using dibromoethane followed by saponification to produce the 6-Cl-indole acid **35**.

### Scheme 3<sup>a</sup>

**Tricyclic Fragment Optimization.** Among the initial hits obtained in the screen, we identified fragments containing a tricyclic indole 2-carboxylic acid that bind to Mcl-1 (Table 1). The thiazine-containing tricyclic fragment **2** displaces a FITC-labeled BAK peptide from Mcl-1 with a  $K_i$  of 35  $\mu$ M in an FPA assay. SAR of the fragment core was investigated by using small tricyclic indoles with substitutions on rings A-C (Table 1) that were either purchased or synthesized as described in Scheme 1.

**Table 1.**

In general, all of the tricyclic indole acids exhibited similar binding affinity for Mcl-1 compared to the initial hit **2** with ligand efficiencies (LE)  $\geq 0.35$ . Both compounds **3** and **4**, containing C-ring moieties showed significantly enhanced binding affinity when compared to the unsubstituted indole 2-carboxylic acid **8**<sup>28</sup>. Improved affinity was also observed by substituting a methyl group at the R<sup>1</sup> (compound **5**, **6**) or R<sup>2</sup> (compound **2**) positions compared to the unsubstituted fragments **3** and **4**, suggesting that additional hydrophobic protein binding pockets may be accessible from these positions. In addition, C-ring analogs containing a thiazine moiety (**3** and **5**) or morpholine (**7**) were potent and preferred over the piperidine analogs **4** and **6**. These results suggest that modifications in the C-ring are not only tolerated but can make additional

interactions with Mcl-1 that result in improvements in binding affinity.

To determine how these tricyclic indole fragments bind to Mcl-1, we performed NMR-based structural studies using compound **2** bound to double-labeled ( $^{15}\text{N}$ ,  $^{13}\text{C}$ ) Mcl-1. Several key NOEs were observed between the indole phenyl ring B and A227, M231, and F270 of Mcl-1. In addition, the thiazine methyl group at  $\text{R}^2$  exhibited weak NOEs involving T266 (Figure 1A). This pattern of intermolecular protein/ligand NOEs strongly suggests that compound **2** and similar analogs bind in the upper part of the second hydrophobic pocket<sup>17</sup>, P2, utilized by peptides that bind to Mcl-1. In peptides, this pocket is occupied by a highly conserved Leu residue.

The NMR-derived structural information was used to generate a model in which the carboxylic acid moiety of compound **2** on ring A points toward R263. In addition, the indole phenyl on ring B points towards A227 and M231 with ring C sitting next to the adjacent hydrophobic pocket (P3) (Figure 1B). This orientation places the indole 3-position ( $\text{R}^1$ ) to point into the lower P2 pocket. Thus, the model structure predicted that the  $\text{R}^1$  position is in an ideal location for extending deep into the pocket.

### Figure 1.

**Fragment Merging with the Tricyclic Scaffold.** We previously discovered that a substantial boost in affinity could be obtained by merging fragments that bind in the upper part of the P2 pocket to fragments that predominantly bind deeper into the pocket than Leu of the BH3 peptide.<sup>28</sup> On the basis of the fragment SAR (Table 1), NMR-derived structural information, and molecular modeling, we designed and synthesized a new series of Mcl-1 inhibitors by merging molecules that bind deep into the P2 pocket to the tricyclic indoles. The binding affinity and selectivity of these compounds for binding to Mcl-1 are shown in Table 2. In an earlier study<sup>28</sup>, we found that both a 1-naphthyl and a 3,5-dimethyl-4-chloro-phenyl fragment bound to the lower



P2 pocket and gave similar affinities for compounds containing both upper and lower P2 pocket binders. To generate the initial SAR in this series, a 1-naphthyl group as the lower P2 pocket binding group was connected to the R<sup>1</sup> position of tricyclic 2-indole carboxylic acid cores bearing thiazine, piperidine or a morpholine C-ring moiety, using either a three- or four-atom linker. As expected, the merged compounds (**16-21**) exhibited markedly enhanced binding affinities compared to the parent compounds (**2-7**) that lack a lower pocket binding group. In particular, compounds containing a four-atom linker (**19, 20** and **21**) showed more than 2 orders of magnitude increased affinity for Mcl-1 compared to the initial fragment **2**. The three-atom linker is not preferred, as compounds **16, 17** and **18** exhibited >10-fold higher *K<sub>i</sub>* values compared to the corresponding four-atom linker analogs. Compounds containing different C-ring moieties had improved affinity from the original fragment and showed a parallel SAR trend with respect to linker length.

**Table 2.**

**Structure of compounds 36 and 37**

**SAR of the C-ring Unit in the Merged Compounds.** The influence of C-ring composition on binding to Mcl-1 was evaluated by preparing compounds **19-25** that contain heterocyclic units with varying ring sizes and functional groups. Similar to that observed for the fragments, the 6-membered C-ring moiety bearing *S*- (**19**) or *O*- (**21**) were slightly preferred to the compounds containing a carbon analog **20**. The 7-membered thiazepine C-ring unit was well tolerated with compound **23** exhibiting near equal potency to the thiazine analog **19**. We also explored the possibility of incorporating polar functional groups within the C-ring component. Interestingly, both sulfoxide and sulfone oxidation states (**22, 24, 25**) showed higher affinity to Mcl-1 than their parent sulfides (**19** or **23**). These observed trends in the SAR for the C-ring moiety were

hypothesized to be advantageous for modulating the drug-like properties of ligands. For example, pharmaceutical agents containing a sulfone functional group generally exhibit more desirable properties, such as higher aqueous solubility and better metabolic stability, than the corresponding sulfide.<sup>35</sup> Compound **25**, the most potent Mcl-1 inhibitor ( $K_i = 61$  nM) in this series, has more than a 5-fold improvement in potency when compared to the analog **36** ( $K_i = 330$  nM)<sup>28</sup>, which contains the unsubstituted indole core lacking the C-ring moiety. These observations strongly suggest that introduction of a proper C-ring group in the series can enhance not only the binding affinity for Mcl-1 but also provides a pharmacophore unit which can be utilized to optimize the pharmaceutical properties of the molecules without sacrificing the potency of the parent ligand.

**Optimization of the P2 Pocket Anchor Group.** To further explore the SAR of the tricyclic indoles, compounds **26-30** were prepared by tethering lower pocket binding units that were identified in our earlier work<sup>28</sup> along with new chemical moieties to the thiazine containing tricyclic indole fragment **3** using optimized four-atom linkers. Bicyclic aromatic P2 binding groups, such as 1'-(5,6,7,8-tetrahydronaphthyl) and 1'-(4'-Cl-naphthyl) contained in compounds **26** and **27**, exhibited comparable potency to the 1-naphthyl analog **19**. Conversely, compound **28** containing 2'-(5,6,7,8-tetrahydronaphthyl) showed a 3-fold reduction in affinity to Mcl-1 compared to its regioisomer **26** and the 1-naphthyl analog **19**, indicating the importance of the attachment position for optimal binding. Compound **29** which contains a 3'-Me-4'-Cl-phenyl group displays a 240-fold improved potency over fragment **3**, and compound **30** bearing a 3',5'-di-Me-4'-Cl-phenyl moiety exhibited the most potent inhibitory activity against Mcl-1 with a  $K_i$  of 71 nM, representing a 720-fold improvement in affinity compared to the core unit **3**.

To further investigate the effect of C-ring variations for compounds containing the 3,5'-di-Me-4'-Cl-phenyl group, compounds **30-33** were prepared. These inhibitors exhibited a parallel SAR trend compared to the corresponding 1-naphthyl analogs **19-21** and **23** with a 1.5–4.3 fold improvement in binding affinity. The thiazepine analog **33** displayed a  $K_i$  value (40 nM) which corresponds to a 7.5-fold increase in binding affinity compared to the indole analog **37** ( $K_i$  = 300 nM), which lacks a C-ring moiety.<sup>28</sup>

**X-Ray structures of the Tricyclic Compounds.** To guide further compound optimization, X-ray co-crystal structures of **17** and **24** complexed with Mcl-1 were obtained (Figure 2A-C). Both compounds **17** and **24** adopt similar binding poses as our earlier benzthiophene analog (PDB: 4HW3). In both structures, the naphthyl group penetrated into the deepest part of the hydrophobic pocket and induced a pronounced bend in helix 4 ( $\alpha$ 4) that likely helps to anchor the unit at this binding sub-site. In addition, the naphthyl group was positioned near F270, which causes favorable edge-to-face CH/ $\pi$  aromatic interactions with the phenyl group of this residue. The top of  $\alpha$ 4 sits close to the ligand causing the loop connecting helix 4-5 to be pulled towards the ligand allowing the carboxylic acid group of the ligand to engage in ion pairing interactions with the guanidinium moiety of R263.

### Figure 2A-C

Interestingly, when the co-crystal structures of **17** and **24** are superimposed, the indole cores and naphthyl groups sit in almost the same position. However, the C-ring units adopt different binding conformations, and the larger thiazepane-oxide ring of **24** causes a pucker that localizes parts of the ring to be closer to A227 and T266 of Mcl-1 (Figure 2A). This may contribute to hydrophobic burial and could explain the slight improvement in binding affinity observed for this inhibitor. Finally, the X-ray structures predict that substitutions at the 6-

position of the indole with small hydrophobic groups could fill the space between the ligands and helix 3 ( $\alpha 3$ ) to gain additional binding affinity (Figure 2B and C).

**Tricyclic Indole Core optimization by Substitutions of the B-Ring.** From our X-ray structures and previously reported SAR<sup>28</sup>, we hypothesized that a substantial increase in binding affinity to Mcl-1 could be obtained by a substitution at the 6-position of the indole of the 6,5-fused heterocyclic carboxylic acid core. In a previously described series of compounds, a 6-Cl-indole addition (as exemplified in compound **1**) exhibited greater than a 5-fold enhanced potency compared to the parent (**37**).<sup>28</sup> To determine if this trend was the same for the tricyclic series, two 6-Cl-tricyclic indoles **34** and **35**, containing piperidine and morpholine C-ring moieties respectively, were evaluated. Indeed, these modifications resulted in a >10-fold increase in binding affinities for both compounds, when compared to the des chloro analogs **31**, **32**. The affinity gain is likely the result of filling the pocket indicated by the arrow in Figure 2 (B,C). Our best inhibitor, **34**, displayed a remarkable 36-fold higher potency over its des-Cl parent (**31**) and had a  $K_i$  of 3 nM and LE = 0.40. These results strongly suggest that binding contributions from the C-ring moiety and the 6-Cl group are additive and can even be synergistic for some combinations.

**Mcl-1 Selectivity.** Excessive inhibition of Bcl-xL in platelets causes mechanism-based, dose-dependent thrombocytopenia in preclinical studies<sup>24,36,37</sup> and in clinical trials of the dual Bcl-2/Bcl-xL inhibitor ABT-263.<sup>24</sup> Therefore, we sought to obtain selective Mcl-1 inhibitors that do not inhibit Bcl-xL to avoid these undesired adverse effects. To evaluate the selectivity of our series, binding affinities to the anti-apoptotic proteins Bcl-xL and Bcl-2 were measured in an FPA assay (Table 2). In all cases, the tricyclic 2-indole carboxylic acids (19-35) containing the 4-atom linker exhibited only weak affinity for both Bcl-xL ( $K_i \geq 1.9 \mu\text{M}$ ) and Bcl-2 ( $K_i \geq 0.77$

1  
2  
3  $\mu\text{M}$ ). Our most potent 6-Cl containing Mcl-1 inhibitors **34** and **35** exhibit >1700-fold binding  
4  
5 selectivity over Bcl-xL and greater than 100-fold selectivity over Bcl-2. All structural  
6  
7 modifications on the series that enhance the affinity for Mcl-1 had relatively little effect on  
8  
9 improving binding to Bcl-xL or Bcl-2. As a result, the compounds became more selective  
10  
11 against Bcl-xL as they became more potent for Mcl-1. Mcl-1 inhibitors likely achieve selectivity  
12  
13 by filling the lower P2 pocket (Figure 2B) which is not present in Bcl-xL (PDB ID : 2YXJ) or  
14  
15 BCL-2 (PDB ID : 4LVT) ligand structures.  
16  
17  
18  
19

20  
21 **Pulldown Experiment.** To determine whether compound **34** could bind to cellular Mcl-1 and  
22  
23 inhibit the binding of a peptide derived from a pro-apoptotic protein<sup>38</sup>, cell lysates from Human  
24  
25 chronic myelogenous leukemia K562 cells were incubated with biotin labeled MS-1, a peptide  
26  
27 that binds specifically to Mcl-1.<sup>39</sup> This peptide selectively pulls down cellular Mcl-1. As shown  
28  
29 in Figure 3, the addition of compound **34** blocks the ability of MS-1 to pulldown Mcl-1,  
30  
31 demonstrating that the compound binds to cellular Mcl-1 and blocks the interaction with biotin  
32  
33 MS-1 in a dose-dependent manner.  
34  
35  
36  
37

## 38 Conclusion

39  
40  
41 We have described the optimization of a novel series of small molecule Mcl-1 inhibitors  
42  
43 based on a hit obtained from an NMR-based fragment screen. NMR-based structural studies and  
44  
45 SAR exploration resulted in a binding affinity increase of 100-fold over the initial micromolar  
46  
47 fragment hit and further optimization, guided by structural data, resulted in an additional 30-fold  
48  
49 gain in affinity. The resulting compound binds to Mcl-1 with a  $K_i = 3 \text{ nM}$ , is selective over Bcl-2  
50  
51 and Bcl-xL, and binds to cellular Mcl-1 to prevent binding of a biotin labeled peptide that binds  
52  
53 specifically to Mcl-1. An important result of this study is that the SAR knowledge learned from  
54  
55  
56  
57  
58  
59  
60

one fragment core could be rapidly translated to other related fragment hits. We were able to rapidly replace the core of our initial indole series<sup>28</sup> with another fragment hit to obtain novel compounds with high Mcl-1 potency and selectivity.

While this manuscript was in review, Leverson *et al* published the characterization of a potent ( $K_i = 0.454$  nM) small molecule inhibitor, A-1210477.<sup>40</sup> This study emphasized the exquisite potency (“subnanomolar and often low picomolar affinities”) needed to demonstrate on-target cellular effects. Therefore, the low nanomolar compounds (e.g. **34**,  $K_i = 3.0$  nM) described here are not expected to display unambiguous on-target cellular activity. However, this tricyclic 2-indole carboxylic acid represents an excellent starting point for additional optimization to achieve these goals.

## EXPERIMENTAL SECTION

### Chemistry

**General.** All NMR spectra were recorded at room temperature on a 400 MHz AMX Bruker spectrometer. <sup>1</sup>H chemical shifts are reported in  $\delta$  values in ppm downfield with the deuterated solvent as the internal standard. Data are reported as follows: chemical shift, multiplicity (s = singlet, d = doublet, t = triplet, q = quartet, br = broad, m = multiplet), integration, coupling constant (Hz). Low resolution mass spectra were obtained on an Agilent 1200 series 6140 mass spectrometer with electrospray ionization. All samples were of  $\geq 95\%$  purity as analyzed by LC–UV/vis-MS. Analytical HPLC was performed on an Agilent 1200 series with UV detection at 214 and 254 nm along with ELSD detection. LC/MS parameters were as follows: Phenomenex-C18 Kinetex column, 50 x 2.1 mm, 2 min gradient, 5% (0.1% TFA/MeCN) / 95% (0.1% TFA/ H<sub>2</sub>O) to 100% (0.1% TFA/MeCN). Preparative purification was performed on a Gilson HPLC (Phenomenex-C18, 100 x 30 mm, 10 min gradient, 5→95% MeCN/H<sub>2</sub>O with

0.1% TFA) or by automated flash column chromatography (Isco, Inc. 100sg Combiflash). Solvents for extraction, washing, and chromatography were HPLC grade. All reagents were purchased from chemical suppliers and used without purification.

**6-Methyl-2,3-dihydro-[1,4]thiazino[2,3,4-hi]indole-5-carboxylic acid (5). General Procedure**

**for the Fischer Indole Reaction.** To a stirred solution of 2,3-dihydro-4H-benzo[b][1,4]thiazin-4-amine (83 mg, 0.50 mmol) in absolute EtOH (2 mL) was added methyl 2-oxobutanoate (58 mg, 0.50 mmol) at 20 °C. The reaction mixture was stirred for 30 min at 50 °C then cooled to 0 °C. Concentrated H<sub>2</sub>SO<sub>4</sub> (0.2 mL) was added dropwise then the reaction mixture was warmed to 50 °C and stirred for an additional 4 h. The reaction mixture was cooled to 20 °C then concentrated *in vacuo*. The residue was dissolved in CH<sub>2</sub>Cl<sub>2</sub> (5 mL), and the organic solution was washed with saturated aqueous NaHCO<sub>3</sub> solution followed by brine, dried over MgSO<sub>4</sub>, filtered, and concentrated *in vacuo*. The residue was dissolved in 1:1 mixture of MeOH/THF (2 mL) then KOH (280 mg, 5.0 mmol) was added. The reaction mixture was stirred for 2 h at 50 °C then concentrated *in vacuo*. The residue was dissolved in H<sub>2</sub>O then acidified to pH 1 with concentrated HCl. The mixture was extracted with EtOAc, dried over MgSO<sub>4</sub>, filtered, and concentrated *in vacuo*. The crude product was purified by reverse phase preparative HPLC (H<sub>2</sub>O/CH<sub>3</sub>CN gradient to 95% CH<sub>3</sub>CN/0.1% TFA) to yield the title compound (103 mg, 0.44 mmol) as a white solid. <sup>1</sup>HNMR(400 MHz, DMSO-*d*<sub>6</sub>): δ (ppm) 7.45 (d, *J* = 8.0 Hz, 1 H), 7.09 (d, *J* = 7.7 Hz, 1H), 7.02 (dd, *J* = 8.0, 7.7 Hz, 1 H), 4.73-4.71 (m, 2 H), 3.32-3.30 (m, 2 H), 2.52 (s, 3 H): >98% at 215 nm, MS (ESI) *m/z* = 234.1 [M + H]<sup>+</sup>.

**1-Methyl-5,6-dihydro-4H-pyrrolo[3,2,1-ij]quinoline-2-carboxylic acid (6).** The general procedure for Fischer indole reaction was followed using 3,4-dihydroquinolin-1(2H)-amine (74 mg, 0.50 mmol) and methyl 2-oxobutanoate (58 mg, 0.50 mmol) to yield the title compound (97

mg, 0.45mmol). <sup>1</sup>HNMR(400 MHz, DMSO-*d*<sub>6</sub>): δ (ppm) 7.45 (dd, *J* = 6.6, 2.6 Hz, 1 H), 7.01-6.96 (m, 2 H), 4.43 (t, *J* = 5.7 Hz, 2 H), 2.91 (t, *J* = 6.1 Hz, 2 H), 2.52 (s, 3 H), 2.15-2.09 (m, 2 H); >98% at 215 nm, MS (ESI) *m/z* = 216.1 [M + H]<sup>+</sup>.

**6-Methyl-2,3-dihydro-[1,4]oxazino[2,3,4-*hi*]indole-5-carboxylic acid (7).** The general procedure for Fischer indole reaction was followed using 2,3-dihydro-4H-benzo[*b*][1,4]oxazin-4-amine (100 mg, 0.66 mmol) and methyl 2-oxobutanoate (85 mg, 0.73 mmol) to yield the title compound (81 mg, 0.37mmol). <sup>1</sup>HNMR(400 MHz, DMSO-*d*<sub>6</sub>): δ (ppm) 7.20 (d, *J* = 8.0 Hz, 1 H), 6.95 (dd, *J* = 8.0, 7.6 Hz, 1H), 6.67 (d, *J* = 7.6 Hz, 1 H), 4.52-4.47 (m, 4 H), 2.52 (s, 3 H); >98% at 215 nm, MS (ESI) *m/z* = 218.1 [M + H]<sup>+</sup>.

**6-(2-(Naphthalen-1-yloxy)ethyl)-2,3-dihydro-[1,4]thiazino[2,3,4-*hi*]indole-5-carboxylic acid (16). General Procedure.** A solution of 2,3-dihydro-4H-benzo[*b*][1,4]thiazin-4-amine (336 mg, 2.0 mmol) and 2-oxopentanedioic acid (325 mg, 2.2 mmol) in EtOH (5 mL) was stirred at 50 °C for 30 min then cooled to 0 °C. To the reaction mixture was added conc. H<sub>2</sub>SO<sub>4</sub> (0.5 mL) dropwise at 0 °C. The reaction mixture was stirred for 2h at 60 °C then quenched by pouring into ice then extracted with CH<sub>2</sub>Cl<sub>2</sub>. The combined organic layer was washed with sat. NaHCO<sub>3</sub>, water, brine, dried over MgSO<sub>4</sub>, filtered and concentrated *in vacuo*. The residue was purified by filtering through a silica gel column using Et<sub>2</sub>O as an eluent. The filtrate was concentrated *in vacuo* to give 1:1 mixture of 6-(2-ethoxy-2-oxoethyl)-2,3-dihydro-[1,4]thiazino[2,3,4-*hi*]indole-5-carboxylic acid and ethyl 6-(2-ethoxy-2-oxoethyl)-2,3-dihydro-[1,4]thiazino[2,3,4-*hi*]indole-5-carboxylate as an off-white solid in 145 mg. This mixture of products was directly used for the subsequent step without further purification.

To a solution of a mixture of products (145 mg) from the previous step in MeOH and benzene mixture (1:10, 2.0 mL) was added TMSCHN<sub>2</sub> (2M in hexane) until bubbling stopped



and a yellow color of the reaction mixture persisted. The reaction mixture was stirred for additional 10 min at 20 °C then concentrated *in vacuo* to give a mixture of methyl and ethyl 6-(2-ethoxy-2-oxoethyl)-2,3-dihydro-[1,4]thiazino[2,3,4-*hi*]indole-5-carboxylate. They were directly used for the subsequent step without further purification.

To a solution of a mixture of methyl and ethyl 6-(2-ethoxy-2-oxoethyl)-2,3-dihydro-[1,4]thiazino[2,3,4-*hi*]indole-5-carboxylate from the previous step in THF (2.0 mL) was added  $\text{BH}_3$  in THF (2 mL, 2 mmol) at 20 °C. The reaction mixture was stirred for 5h at 20 °C and quenched by addition of MeOH then concentrated *in vacuo*. The residue was purified by flash chromatography (Combi-flash Rf Hexane/EtOAc gradient 0-100%) to give a mixture of methyl and ethyl 6-(2-hydroxyethyl)-2,3-dihydro-[1,4]thiazino[2,3,4-*hi*]indole-5-carboxylate as a colorless oil in 110 mg (0.40 mmol).

To a solution of a mixture of methyl and ethyl 6-(2-hydroxyethyl)-2,3-dihydro-[1,4]thiazino[2,3,4-*hi*]indole-5-carboxylate (50 mg, 0.18 mmol),  $\text{PPh}_3$  (71 mg, 0.27 mmol) and naphthalen-1-ol (44 mg, 0.28mmol) in THF (1.0 mL) was added Dt-BuAD (62 mg, 0.27 mmol) at 20 °C. The reaction mixture was stirred for 15h at 20 °C. To the reaction mixture was added KOH (101 mg, 10 mmol) and MeOH (1.0 mL). The reaction mixture was stirred for 2h at 65 °C then concentrated *in vacuo*. The crude product was purified by reverse phase preparative HPLC (Phenomenex Gemini C18,  $\text{H}_2\text{O}/\text{CH}_3\text{CN}$  gradient to 95%  $\text{CH}_3\text{CN}$  0.1% TFA) to yield the title compound (43 mg, 0.11 mmol) as a light yellow solid.  $^1\text{H}$ NMR(400 MHz,  $\text{DMSO}-d_6$ ):  $\delta$  8.07 (d,  $J = 8.4$  Hz, 1 H), 7.82(d,  $J = 8.0$ , Hz, 1H), 7.68 (dd,  $J = 7.4$ , 1.6 Hz, 1H), 7.49 (dd,  $J = 6.9$ , 1.6 Hz, 1H), 7.47-7.34 (comp, 3H), 7.14-7.08 (comp, 2H), 6.96 (d,  $J = 7.3$  Hz, 1H), 4.77-4.74 (m, 2H), 4.36 (t,  $J = 6.6$  Hz, 2H), 3.68 (t,  $J = 6.7$  Hz, 2H), 3.35-3.10 (m, 2H); >98% at 215 nm, MS (ESI)  $m/z = 390.1$   $[\text{M} + \text{H}]^+$ .

**1-(2-(Naphthalen-1-yloxy)ethyl)-5,6-dihydro-4*H*-pyrrolo[3,2,1-*ij*]quinoline-2-carboxylic acid (17).** The title compound was prepared as a white solid according to procedures described for preparing compound 16 by substituting 2,3-dihydro-4*H*-benzo[*b*][1,4]thiazin-4-amine with 3,4-dihydroquinolin-1(2*H*)-amine in 23% overall yield. <sup>1</sup>H NMR (400 MHz, DMSO-*d*<sub>6</sub>) δ 8.10 (d, *J* = 8.3 Hz, 1H), 7.83 (d, *J* = 8.1 Hz, 1H), 7.67 (dd, *J* = 7.7, 1.5 Hz, 1H), 7.49 (ddd, *J* = 8.2, 6.8, 1.3 Hz, 1H), 7.45 – 7.31 (m, 3H), 7.10 – 7.00 (m, 2H), 6.96 (d, *J* = 7.5 Hz, 1H), 4.50 – 4.42 (m, 2H), 4.35 (t, *J* = 6.7 Hz, 2H), 3.67 (t, *J* = 6.7 Hz, 2H), 2.92 (t, *J* = 6.1 Hz, 2H), 2.18 – 2.04 (m, 2H); >98% at 215 nm, MS (ESI) *m/z* = 372.2 [M + H]<sup>+</sup>.

**6-(2-(Naphthalen-1-yloxy)ethyl)-2,3-dihydro-[1,4]oxazino[2,3,4-*hi*]indole-5-carboxylic acid (18).** The title compound was prepared as a white solid according to procedures described for preparing compound 16 by substituting 2,3-dihydro-4*H*-benzo[*b*][1,4]thiazin-4-amine with 2,3-dihydro-4*H*-benzo[*b*][1,4]oxazin-4-amin in 18% overall yield. <sup>1</sup>H NMR (400 MHz, DMSO-*d*<sub>6</sub>) δ 8.09 (d, *J* = 8.1 Hz, 1H), 7.83 (d, *J* = 8.1 Hz, 1H), 7.51 - 7.46 (m, 1H), 7.45 - 7.32 (m, 4H), 7.02 (t, *J* = 7.9 Hz, 1H), 6.96 (d, *J* = 7.5 Hz, 1H), 6.71 (d, *J* = 7.3 Hz, 1H), 4.57 (t, *J* = 4.7 Hz, 2H), 4.48 (t, *J* = 4.6 Hz, 2H), 4.37 (t, *J* = 6.8 Hz, 2H), 3.67 (t, *J* = 6.7 Hz, 2H); >98% at 215 nm, MS (ESI) *m/z* = 374.1 [M + H]<sup>+</sup>.

**6-(3-(Naphthalen-1-yloxy)propyl)-2,3-dihydro-[1,4]thiazino[2,3,4-*hi*]indole-5-carboxylic acid (19).** A mixture of methyl and ethyl 6-(3-hydroxypropyl)-2,3-dihydro-[1,4]thiazino[2,3,4-*hi*]indole-5-carboxylate (465 mg, 1.6 mmol) was prepared as a yellow oil according to procedures described for preparing compound 16 using 2,3-dihydro-4*H*-benzo[*b*][1,4]thiazin-4-amine (500 mg, 3.0 mmol) and 2-oxohexanedioic acid (722 mg, 4.5 mmol) in 53% overall yield.

The title compound was prepared (25 mg, 0.062 mmol) as an off-white solid following the Mitsunobu reaction procedure described for preparing compound 16 using a mixture of

methyl and ethyl 6-(3-hydroxypropyl)-2,3-dihydro-[1,4]thiazino[2,3,4-*hi*]indole-5-carboxylate (56 mg, 0.2 mmol). <sup>1</sup>H NMR (400 MHz, DMSO-*d*<sub>6</sub>) δ 8.21 – 8.15 (m, 1H), 7.90 – 7.82 (m, 1H), 7.57 – 7.34 (m, 5H), 7.06 (d, *J* = 7.2 Hz, 1H), 6.97 – 6.84 (m, 2H), 4.77 – 4.67 (m, 2H), 4.17 (t, *J* = 6.0 Hz, 2H), 3.32 – 3.28 (m, 4H), 2.25 – 2.14 (m, 2H); >98% at 215 nm, MS (ESI) *m/z* = 404.1 [M + H]<sup>+</sup>.

**1-(3-(Naphthalen-1-yloxy)propyl)-5,6-dihydro-4*H*-pyrrolo[3,2,1-*ij*]quinoline-2-carboxylic acid (20).** A mixture of methyl and ethyl 1-(3-hydroxypropyl)-5,6-dihydro-4*H*-pyrrolo[3,2,1-*ij*]quinoline-2-carboxylate (72 mg, 0.25 mmol) was prepared as a pale yellow oil according to procedures described for preparing compound 16 using 3,4-dihydroquinolin-1(2*H*)-amine (74 mg, 0.50 mmol) and 2-oxohexanedioic acid (160 mg, 1.0 mmol) in 50% overall yield.

The title compound was prepared (20 mg, 0.052 mmol) as an off-white solid following the Mitsunobu reaction procedure described for preparing compound 16 using a mixture of methyl and ethyl 1-(3-hydroxypropyl)-5,6-dihydro-4*H*-pyrrolo[3,2,1-*ij*]quinoline-2-carboxylate (55 mg, 0.2 mmol). <sup>1</sup>H NMR (400 MHz, DMSO-*d*<sub>6</sub>) δ 8.24 – 8.17 (m, 1H), 7.89 – 7.85 (m, 1H), 7.56 – 7.41 (m, 4H), 7.38 (t, *J* = 7.9 Hz, 1H), 6.97 (d, *J* = 6.9 Hz, 1H), 6.91 – 6.84 (m, 2H), 4.48 – 4.40 (m, 2H), 4.16 (t, *J* = 6.1 Hz, 2H), 3.32 – 3.30 (m, 2H), 2.91 (t, *J* = 6.1 Hz, 2H), 2.25 – 2.06 (m, 4H); >98% at 215 nm, MS (ESI) *m/z* = 386.2 [M + H]<sup>+</sup>.

**6-(3-(Naphthalen-1-yloxy)propyl)-2,3-dihydro-[1,4]oxazino[2,3,4-*hi*]indole-5-carboxylic acid (21).** A mixture of methyl and ethyl 6-(3-hydroxypropyl)-2,3-dihydro-[1,4]oxazino[2,3,4-*hi*]indole-5-carboxylate (375 mg, 1.3 mmol) was prepared as a pale yellow oil according to procedures described for preparing compound 16 using 2,3-dihydro-4*H*-benzo[*b*][1,4]oxazin-4-amin (430 mg, 2.90 mmol) and 2-oxohexanedioic acid (595 mg, 3.7 mmol) in 45% overall yield.

The title compound was prepared (55 mg, 0.15 mmol) as an off-white solid following the Mitsunobu reaction procedure described for preparing compound 16 using a mixture of methyl and ethyl 6-(3-hydroxypropyl)-2,3-dihydro-[1,4]oxazino[2,3,4-*hi*]indole-5-carboxylate (75 mg, 0.27 mmol). <sup>1</sup>H NMR (400 MHz, DMSO-*d*<sub>6</sub>) δ 8.18 (dd, *J* = 7.7, 1.8 Hz, 1H), 7.86 (dd, *J* = 7.4, 1.9 Hz, 1H), 7.56 - 7.42 (m, 3H), 7.38 (dd, *J* = 8.0, 7.6 Hz, 1H), 7.22 (d, *J* = 8.0 Hz, 1H), 6.91 - 6.82 (m, 2H), 6.65 (d, *J* = 7.4 Hz, 1H), 4.54 (t, *J* = 4.6 Hz, 2H), 4.47 (t, *J* = 4.8 Hz, 2H), 4.17 (t, *J* = 6.0 Hz, 2H), 3.36 - 3.31 (m, 2H), 2.26 - 2.17 (m, 2H); >98% at 215 nm, MS (ESI) *m/z* = 388.1 [M + H]<sup>+</sup>.

**6-(3-(naphthalen-1-yloxy)propyl)-2,3-dihydro-[1,4]thiazino[2,3,4-*hi*]indole-5-carboxylic acid 1,1-dioxide (22).** To a solution of 6-(3-(naphthalen-1-yloxy)propyl)-2,3-dihydro-[1,4]thiazino[2,3,4-*hi*]indole-5-carboxylic acid (20 mg, 0.050 mmol) in CH<sub>2</sub>Cl<sub>2</sub> (1.0 mL) and THF (1.0 mL) was added *m*-CPBA (17 mg (77% pure), 1.0 mmol) at 20 °C. The reaction mixture was stirred for 1 h at 20 °C then quenched by addition of H<sub>2</sub>O, extracted with CH<sub>2</sub>Cl<sub>2</sub> and concentrated *in vacuo*. The residue was purified by reverse-phase preparative HPLC (Phenomenex Gemini C18, H<sub>2</sub>O/CH<sub>3</sub>CN gradient to 25-95% CH<sub>3</sub>CN 0.1% TFA) to give the title compound (12 mg, 0.028 mmol) as a white solid. <sup>1</sup>H NMR (400 MHz, DMSO-*d*<sub>6</sub>) δ 8.13 (dd, *J* = 8.6, 1.8 Hz, 1H), 8.03 (d, *J* = 8.1 Hz, 1H), 7.89 - 7.83 (m, 1H), 7.72 (d, *J* = 7.4 Hz, 1H), 7.58 - 7.42 (m, 3H), 7.41 - 7.33 (m, 1H), 7.21 (t, *J* = 7.8 Hz, 1H), 6.88 (d, *J* = 7.3 Hz, 1H), 5.09 - 4.93 (m, 2H), 4.17 (t, *J* = 6.0 Hz, 2H), 3.91 - 3.80 (m, 2H), 3.41 - 3.35 (m, 2H), 2.29 - 2.14 (m, 2H); >98% at 215 nm, MS (ESI) *m/z* = 436.1 [M + H]<sup>+</sup>.

**7-(3-(Naphthalen-1-yloxy)propyl)-3,4-dihydro-2H-[1,4]thiazepino[2,3,4-*hi*]indole-6-carboxylic acid (23).** A mixture of methyl and ethyl 7-(3-hydroxypropyl)-3,4-dihydro-2H-[1,4]thiazepino[2,3,4-*hi*]indole-6-carboxylate (211 mg, 0.72 mmol) was prepared as a pale

yellow oil according to procedures described for preparing compound 16 using 2,3-dihydro-4*H*-benzo[*b*][1,4]oxazin-4-amin (261 mg, 1.45 mmol) and 2-oxohexanedioic acid (301 mg, 1.88 mmol) in 50% overall yield.

The title compound was prepared (76 mg, 0.18 mmol) as a white solid following the Mitsunobu reaction procedure described for preparing compound 16 using a mixture of methyl and ethyl 7-(3-hydroxypropyl)-3,4-dihydro-2*H*-[1,4]thiazepino[2,3,4-*hi*]indole-6-carboxylate (63 mg, 0.20 mmol). <sup>1</sup>H NMR (400 MHz, DMSO-*d*<sup>6</sup>) δ 8.18 (dd, *J* = 7.6, 1.9 Hz, 1H), 7.86 (dd, *J* = 7.3, 2.0 Hz, 1H), 7.61 - 7.42 (m, 4H), 7.38 (dd, *J* = 8.0, 7.8 Hz, 1H), 7.10 (d, *J* = 7.3 Hz, 1H), 6.86 (dd, *J* = 8.0, 7.7 Hz, 2H), 4.86 (t, *J* = 5.8 Hz, 2H), 4.16 (t, *J* = 6.0 Hz, 2H), 3.34 (t, *J* = 6.6 Hz, 2H), 3.24 (t, *J* = 6.6 Hz, 2H), 2.34 - 2.23 (m, 2H), 2.22 - 2.13 (m, 2H); >98% at 215 nm, MS (ESI) *m/z* = 418.1 [M + H]<sup>+</sup>.

**7-(3-(Naphthalen-1-yloxy)propyl)-3,4-dihydro-2*H*-[1,4]thiazepino[2,3,4-*hi*]indole-6-carboxylic acid 1-oxide (24).** To a cooled (-78 °C) solution of 7-(3-(naphthalen-1-yloxy)propyl)-3,4-dihydro-2*H*-[1,4]thiazepino[2,3,4-*hi*]indole-6-carboxylic acid (35 mg, 0.084 mmol) in THF/CH<sub>2</sub>Cl<sub>2</sub> (1 mL, 1:1) was added *m*-CPBA (19 mg, 0.084 mmol), and the mixture was stirred for 1 h at -78 °C. The reaction was quenched by addition of saturated aqueous NaHCO<sub>3</sub> solution (0.5 mL) followed by H<sub>2</sub>O (12 mL). The quenched reaction mixture was extracted with CH<sub>2</sub>Cl<sub>2</sub> (2x10 mL), dried over Na<sub>2</sub>SO<sub>4</sub>, filtered and concentrated *in vacuo*. The residue was purified by reverse-phase preparative HPLC (Phenomenex Gemini C18, H<sub>2</sub>O/CH<sub>3</sub>CN gradient to 30-80% CH<sub>3</sub>CN 0.1% TFA) to give the title compound (33 mg, 0.076 mmol) as a white amorphous solid. <sup>1</sup>H NMR (400 MHz, DMSO-*d*<sup>6</sup>) δ 8.15 (dd, *J* = 7.6, 1.7 Hz, 1H), 7.91 (d, *J* = 8.0 Hz, 1H), 7.86 (dd, *J* = 7.5, 1.7 Hz, 1H), 7.61 (d, *J* = 7.3 Hz, 1H), 7.57 - 7.42 (m, 3H), 7.38 (dd, *J* = 8.0, 7.6 Hz, 1H), 7.16 (dd, *J* = 7.8, 7.6 Hz, 1H), 6.88 (d, *J* = 7.4, 1H), 4.73

(dt,  $J = 9.1, 4.2$  Hz, 1H), 4.64 (dt,  $J = 9.1, 4.2$  Hz, 1H), 4.18 (t,  $J = 5.9$  Hz, 2H), 3.55 - 3.48 (m, 2H), 3.39 - 3.24 (m, 2H), 3.05 (dt,  $J = 7.3, 6.8$  Hz, 1H), 2.73 - 2.57 (m, 1H), 2.29 - 2.13 (m, 2H); >98% at 215 nm, MS (ESI)  $m/z = 434.1$   $[M + H]^+$ .

**7-(3-(Naphthalen-1-yloxy)propyl)-3,4-dihydro-2H-[1,4]thiazepino[2,3,4-*hi*]indole-6-carboxylic acid 1,1-dioxide (25).** To a cooled solution (0 °C) of 7-(3-(naphthalen-1-yloxy)propyl)-3,4-dihydro-2H-[1,4]thiazepino[2,3,4-*hi*]indole-6-carboxylic acid (15 mg, 0.036 mmol) in  $\text{CH}_2\text{Cl}_2$  (1 mL) was added *m*-CPBA (18 mg, 0.072 mmol), and the mixture was stirred for 2 h at 0 °C. The reaction was quenched by addition of saturated aqueous  $\text{NaHCO}_3$  solution (2 mL). The quenched reaction mixture was extracted with  $\text{CH}_2\text{Cl}_2$  (3x10 mL), dried over  $\text{Na}_2\text{SO}_4$ , filtered and concentrated *in vacuo*. The residue was purified by reverse-phase preparative HPLC (Phenomenex Gemini C18,  $\text{H}_2\text{O}/\text{CH}_3\text{CN}$  gradient to 30-85%  $\text{CH}_3\text{CN}$  0.1% TFA) to give the title compound (14 mg, 0.031 mmol) as an off-white amorphous solid.  $^1\text{H}$  NMR (400 MHz,  $\text{DMSO-}d^6$ )  $\delta$  8.14 (dd,  $J = 7.8, 1.5$  Hz, 1H), 8.06 (d,  $J = 8.0$  Hz, 1H), 7.86 (dd,  $J = 7.4, 1.6$  Hz, 1H), 7.82 (dd,  $J = 7.5, 1.0$  Hz, 1H), 7.59 - 7.42 (m, 3H), 7.38 (dd,  $J = 8.1, 7.7$  Hz, 1H), 7.22 (dd,  $J = 7.8, 7.6$  Hz, 1H), 6.88 (d,  $J = 7.2$  Hz, 1H), 4.89 - 4.68 (m, 2H), 4.18 (t,  $J = 5.9$  Hz, 2H), 3.77 (t,  $J = 6.8$  Hz, 2H), 3.33 (t,  $J = 7.1$  Hz, 2H), 2.42 - 2.28 (m, 2H), 2.27 - 2.12 (m, 2H); >98% at 215 nm, MS (ESI)  $m/z = 450.1$   $[M + H]^+$ .

Compounds 26–33 were prepared following the general procedure outlined above in library format. Purity of all final compounds was determined by HPLC analysis and is >95%. All compounds were isolated as solids.

**6-(3-((5,6,7,8-Tetrahydronaphthalen-1-yl)oxy)propyl)-2,3-dihydro-[1,4]thiazino[2,3,4-*hi*]indole-5-carboxylic acid (26).** Coupling of a mixture of methyl and ethyl 6-(3-

hydroxypropyl)-2,3-dihydro-[1,4]thiazino[2,3,4-*hi*]indole-5-carboxylate and 5,6,7,8-tetrahydronaphthalen-1-ol followed by saponification yielded 26. >98% at 215 nm, MS (ESI)  $m/z = 408.2 [M + H]^+$ .

**6-(3-((4-Chloronaphthalen-1-yl)oxy)propyl)-2,3-dihydro-[1,4]thiazino[2,3,4-*hi*]indole-5-carboxylic acid (27).** Coupling of a mixture of methyl and ethyl 6-(3-hydroxypropyl)-2,3-dihydro-[1,4]thiazino[2,3,4-*hi*]indole-5-carboxylate and 4-chloronaphthalen-1-ol followed by saponification yielded 27. >98% at 215 nm, MS (ESI)  $m/z = 438.1 [M + H]^+$ .

**6-(3-((5,6,7,8-Tetrahydronaphthalen-2-yl)oxy)propyl)-2,3-dihydro-[1,4]thiazino[2,3,4-*hi*]indole-5-carboxylic acid (28).** Coupling of a mixture of methyl and ethyl 6-(3-hydroxypropyl)-2,3-dihydro-[1,4]thiazino[2,3,4-*hi*]indole-5-carboxylate and 5,6,7,8-tetrahydronaphthalen-2-ol followed by saponification yielded 28. >98% at 215 nm, MS (ESI)  $m/z = 408.1 [M + H]^+$ .

**6-(3-(4-Chloro-3-methylphenoxy)propyl)-2,3-dihydro-[1,4]thiazino[2,3,4-*hi*]indole-5-carboxylic acid (29).** Coupling of a mixture of methyl and ethyl 6-(3-hydroxypropyl)-2,3-dihydro-[1,4]thiazino[2,3,4-*hi*]indole-5-carboxylate and 4-chloro-3-methylphenol followed by saponification yielded 29. >98% at 215 nm, MS (ESI)  $m/z = 402.1 [M + H]^+$ .

**6-(3-(4-chloro-3,5-dimethylphenoxy)propyl)-2,3-dihydro-[1,4]thiazino[2,3,4-*hi*]indole-5-carboxylic acid (30).** Coupling of a mixture of methyl and ethyl 6-(3-hydroxypropyl)-2,3-dihydro-[1,4]thiazino[2,3,4-*hi*]indole-5-carboxylate and 4-chloro-3,5-dimethylphenol followed by saponification yielded 30. >98% at 215 nm, MS (ESI)  $m/z = 416.1 [M + H]^+$ .

**1-(3-(4-Chloro-3,5-dimethylphenoxy)propyl)-5,6-dihydro-4*H*-pyrrolo[3,2,1-*ij*]quinoline-2-carboxylic acid (31).** Coupling of a mixture of methyl and ethyl 1-(3-hydroxypropyl)-5,6-dihydro-4*H*-pyrrolo[3,2,1-*ij*]quinoline-2-carboxylate and 4-chloro-3,5-dimethylphenol followed by saponification yielded 31. <sup>1</sup>H NMR (400 MHz, DMSO-*d*<sub>6</sub>) δ 7.43 (d, *J* = 7.6 Hz, 1H), 7.00 - 6.90 (m, 2H), 6.74 (s, 2H), 4.43 (t, *J* = 5.6 Hz, 2H), 3.92 (t, *J* = 6.4 Hz, 2H), 3.17 (t, *J* = 7.2 Hz, 2H), 2.91 (t, *J* = 5.9 Hz, 2H), 2.27 (s, 6H), 2.17 - 2.08 (m, 2H), 2.07 - 1.96 (m, 2H); >98% at 215 nm, MS (ESI) *m/z* = 398.2 [M + H]<sup>+</sup>.

**6-(3-(4-Chloro-3,5-dimethylphenoxy)propyl)-2,3-dihydro-[1,4]oxazino[2,3,4-*hi*]indole-5-carboxylic acid (32).** Coupling of a mixture of methyl and ethyl 6-(3-hydroxypropyl)-2,3-dihydro-[1,4]oxazino[2,3,4-*hi*]indole-5-carboxylate and 4-chloro-3,5-dimethylphenol followed by saponification yielded 32. >98% at 215 nm, MS (ESI) *m/z* = 400.1 [M + H]<sup>+</sup>.

**7-(3-(4-Chloro-3,5-dimethylphenoxy)propyl)-3,4-dihydro-2*H*-[1,4]thiazepino[2,3,4-*hi*]indole-6-carboxylic acid (33).** Coupling of a mixture of methyl and ethyl 7-(3-hydroxypropyl)-3,4-dihydro-2*H*-[1,4]thiazepino[2,3,4-*hi*]indole-6-carboxylate and 4-chloro-3,5-dimethylphenol followed by saponification yielded 33. <sup>1</sup>H NMR (400 MHz, DMSO-*d*<sub>6</sub>) δ 7.46 (d, *J* = 8.0 Hz, 1H), 7.13 (d, *J* = 7.2 Hz, 1H), 6.91 (t, *J* = 7.6 Hz, 1H), 6.75 (s, 2H), 4.90 - 4.81 (m, 2H), 3.94 (t, *J* = 6.3 Hz, 2H), 3.39 - 3.34 (m, 2H), 3.13 - 3.07 (m, 2H), 2.34 - 2.22 (m, 8H), 2.04 - 1.95 (m, 2H); >98% at 215 nm, MS (ESI) *m/z* = 430.1 [M + H]<sup>+</sup>.

**7-chloro-1-(3-(4-chloro-3,5-dimethylphenoxy)propyl)-5,6-dihydro-4*H*-pyrrolo[3,2,1-*ij*]quinoline-2-carboxylic acid (34).** To a stirring mixture of 2-bromo-3-chloroaniline (4.1 g, 20 mmol) in 1M HCl (25 mL) and water (5 mL) at 0 °C was added NaNO<sub>2</sub> (1.38 g, 20 mmol) in water (20 mL), NaCH<sub>3</sub>COOH (9.23 g, 112 mmol) in water (25 mL) and ethyl 2-oxocyclopentane



1  
2  
3  
4  
5  
6  
7  
8  
9  
10  
11  
12  
13  
14  
15  
16  
17  
18  
19  
20  
21  
22  
23  
24  
25  
26  
27  
28  
29  
30  
31  
32  
33  
34  
35  
36  
37  
38  
39  
40  
41  
42  
43  
44  
45  
46  
47  
48  
49  
50  
51  
52  
53  
54  
55  
56  
57  
58  
59  
60  
carboxylate (3.0 mL, 20 mmol) in sequence. The reaction mixture was stirred for 15 min at 0 °C then warmed to 20 °C over 2h and extracted with CH<sub>2</sub>Cl<sub>2</sub>, dried over MgSO<sub>4</sub>, filtered and concentrated *in vacuo* to give 5-(2-(2-bromo-3-chlorophenyl)hydrazono)-6-ethoxy-6-oxohexanoic acid as a red oil in 7.0 g (90% crude).

To a solution of 5-(2-(2-bromo-3-chlorophenyl)hydrazono)-6-ethoxy-6-oxohexanoic acid (7.0 g, 18 mmol) in EtOH (30 mL) was added conc. H<sub>2</sub>SO<sub>4</sub> (7.5 mL), slowly. The reaction mixture was refluxed for 1.5 h. The reaction was quenched by pouring into ice then extracted with CH<sub>2</sub>Cl<sub>2</sub>. The combined organic layer was washed with saturated aqueous NaHCO<sub>3</sub> solution, H<sub>2</sub>O, brine, dried over MgSO<sub>4</sub>, filtered and concentrated *in vacuo*. The residue was purified by flash chromatography (Combi-flash Rf Hex/EtOAc 0-25% gradient) to give ethyl 7-bromo-6-chloro-3-(3-ethoxy-3-oxopropyl)-1*H*-indole-2-carboxylate (4.8 g, 12 mmol) as an off-white solid. MS (ESI) *m/z* = 402.0 [M + H]<sup>+</sup>.

To a solution of ethyl 7-bromo-6-chloro-3-(3-ethoxy-3-oxopropyl)-1*H*-indole-2-carboxylate (2.0 g, 4.8 mmol) in THF (20 mL) was added BH<sub>3</sub> in THF (20 mL, 20 mmol) at 20 °C. The reaction mixture was stirred for 15h at 20 °C and quenched by addition of MeOH then concentrated *in vacuo*. The residue was purified by flash chromatography (Combi-flash Rf Hexane/EtOAc gradient 0-50%) to give ethyl 7-bromo-6-chloro-3-(3-hydroxypropyl)-1*H*-indole-2-carboxylate (1.44 g, 4.0 mmol) as a white solid. MS (ESI) *m/z* = 360.0 [M + H]<sup>+</sup>.

To a solution of ethyl 7-bromo-6-chloro-3-(3-hydroxypropyl)-1*H*-indole-2-carboxylate (1.0 g, 0.28 mmol), PPh<sub>3</sub> (1.1 g, 5.1 mmol) and 3,5-diMe-4-Cl-phenol (810 g, 5.2 mmol) in THF (35 mL) was added Dt-BuAD (990 mg, 5.1 mmol) at 20 °C. The reaction mixture was stirred for 15h at 20 °C then concentrated *in vacuo*. The residue was purified by flash chromatography

(Combi-flash Rf Hexane/EtOAc gradient 0-10%) to give ethyl 7-bromo-6-chloro-3-(3-(4-chloro-3,5-dimethylphenoxy)propyl)-1*H*-indole-2-carboxylate (1.15 g, 2.3 mmol) as a white solid. MS (ESI)  $m/z = 498.0$   $[M + H]^+$ .

To A solution of ethyl 7-bromo-6-chloro-3-(3-(4-chloro-3,5-dimethylphenoxy)propyl)-1*H*-indole-2-carboxylate (100 mg, 0.20 mmol) and 3-bromoprop-1-ene (0.026 mL, 0.30 mmol) in DMF (1.5 mL) was added  $\text{Cs}_2\text{CO}_3$  (196 mg, 0.60 mmol), and the mixture was stirred for 3 h at 80 °C. The reaction mixture was cooled to 20 °C then concentrated *in vacuo*. The residue was purified by flash chromatography (Combi-flash Rf Hexane/EtOAc gradient 0-70%) to give ethyl 1-allyl-7-bromo-6-chloro-3-(3-(4-chloro-3,5-dimethylphenoxy)propyl)-1*H*-indole-2-carboxylate (105 mg 0.19 mmol) as a yellow oil. MS (ESI)  $m/z = 538.1$   $[M + H]^+$ .

To a solution of ethyl 1-allyl-7-bromo-6-chloro-3-(3-(4-chloro-3,5-dimethylphenoxy)propyl)-1*H*-indole-2-carboxylate (105 mg, 0.19 mmol) and  $\text{Bu}_3\text{SnH}$  (0.105 mL, 0.39 mmol) in toluene (1.0 mL) was added AIBN (1.6 mg, 9.7  $\mu\text{mol}$ ), and the mixture was stirred for 90 min at 100 °C. The reaction mixture was cooled to 20 °C then concentrated *in vacuo*. The residue was dissolved in THF (1 mL) and LiOH (0.5 mL, 2N) was added. The reaction mixture was stirred for 24 h at 40 °C then 20 °C then concentrated *in vacuo*. The residue was purified by reverse-phase preparative HPLC (Phenomenex Gemini C18,  $\text{H}_2\text{O}/\text{CH}_3\text{CN}$  gradient to 60-95%  $\text{CH}_3\text{CN}$  0.1% TFA) to give the title compound (41 mg, 0.095 mmol) as a white solid.  $^1\text{H}$  NMR (400 MHz,  $\text{DMSO}-d_6$ )  $\delta$  7.48 (d,  $J = 8.0$  Hz, 1 H), 7.00 (d,  $J = 8.0$  Hz, 1 H), 6.73 (s, 2 H), 4.42 (t,  $J = 6.0$  Hz, 2 H), 3.91 (t,  $J = 6.0$  Hz, 2 H), 3.15 (t,  $J = 6.0$  Hz, 2 H), 2.90 (t,  $J = 6.0$  Hz, 2 H), 2.27 (s, 6 H), 2.15 (m, 2 H), 2.00 (m, 2 H); >98% at 215 nm, MS (ESI)  $m/z = 432.1$   $[M + H]^+$ .

**9-Chloro-6-(3-(4-chloro-3,5-dimethylphenoxy)propyl)-2,3-dihydro-[1,4]oxazino[2,3,4-*hi*]indole-5-carboxylic acid (35).** A solution of ethyl 7-bromo-6-chloro-3-(3-(4-chloro-3,5-dimethylphenoxy)propyl)-1*H*-indole-2-carboxylate (250 mg, 0.50 mmol) and bis(pinacolato)diboron (153 mg, 0.60 mmol) in DMF (2.5 mL) was degased at 20 °C then potassium acetate (226 mg, 2.3 mmol) and 1,1'-bis(diphenylphosphino)ferrocenedichloro palladium(ii) dichloromethane complex (18.32 mg, 0.025 mmol) was added. The reaction mixture was stirred for 20 h at 90 °C under Ar then cooled to 20 °C and diluted with Et<sub>2</sub>O (100 mL). The combined organic solution was washed with H<sub>2</sub>O (4 x 10 mL), brine (10 mL), dried over MgSO<sub>4</sub>, filtered and concentrated *in vacuo*. The residue was purified by flash chromatography (Combi-flash Rf Hexane/EtOAc gradient 0-15%) to give ethyl 6-chloro-3-(3-(4-chloro-3,5-dimethylphenoxy)propyl)-7-(4,4,5,5-tetramethyl-1,3,2-dioxaborolan-2-yl)-1*H*-indole-2-carboxylate (115 mg, 0.21 mmol) as a white solid. MS (ESI) *m/z* = 546.0 [M + H]<sup>+</sup>.

To a solution of ethyl 6-chloro-3-(3-(4-chloro-3,5-dimethylphenoxy)propyl)-7-(4,4,5,5-tetramethyl-1,3,2-dioxaborolan-2-yl)-1*H*-indole-2-carboxylate (63 mg, 0.12 mmol) in THF (1.2 mL) was added 0.5 M NaOH aqueous solution (1.2 mL, 0.60 mmol) followed by 30% H<sub>2</sub>O<sub>2</sub> (118 μL, 1.2 mmol) at 20 °C. The reaction mixture was stirred for 15 h at 20 °C then quenched with sat NH<sub>4</sub>Cl/NH<sub>4</sub>OH buffer solution. The mixture was extracted with EtOAc (2 x 10 mL), dried over MgSO<sub>4</sub>, filtered and concentrated *in vacuo*. The residue was purified by reverse-phase preparative HPLC (Phenomenex Gemini C18, H<sub>2</sub>O/CH<sub>3</sub>CN gradient to 5-65% CH<sub>3</sub>CN 0.1% TFA) to give ethyl 6-chloro-3-(3-(4-chloro-3,5-dimethylphenoxy)propyl)-7-hydroxy-1*H*-indole-2-carboxylate (15 mg, 0.034 mmol). MS (ESI) *m/z* = 436.0 [M + H]<sup>+</sup>.

A mixture of ethyl 6-chloro-3-(3-(4-chloro-3,5-dimethylphenoxy)propyl)-7-hydroxy-1*H*-indole-2-carboxylate (10 mg, 0.023 mmol), cesium carbonate (37 mg, 0.12 mmol) and

dibromoethane (4.0  $\mu$ L, 0.046 mmol) in DMF (460  $\mu$ L) was stirred at 100 °C for 15 h. The mixture was cooled to 20 °C, filtered through a hydrophobic frit and concentrated *in vacuo*. The residue was dissolved in THF (230  $\mu$ L) and 2N aqueous LiOH solution (115  $\mu$ L, 0.23 mmol) was added. The reaction mixture was stirred for 15 h 20 °C, acidified with TFA and concentrated *in vacuo*. The residue was purified by reverse-phase preparative HPLC (Phenomenex Gemini C18, H<sub>2</sub>O/CH<sub>3</sub>CN gradient to 50-95% CH<sub>3</sub>CN 0.1% TFA) to give the title compound (7.5 mg, 0.017 mmol) as a white solid. <sup>1</sup>H NMR (400 MHz, DMSO-*d*<sub>6</sub>)  $\delta$  7.23 (d, *J* = 8.6 Hz, 1H), 6.98 (d, *J* = 8.6 Hz, 1H), 6.71 (s, 2H), 4.57 (m, 4H), 3.93 (t, *J* = 6.2 Hz, 2H), 3.31 (s, 3H), 3.15 (t, *J* = 7.6 Hz, 2H), 2.25 (s, 6H), 2.00 (t, *J* = 7.1 Hz, 2H); >98% at 215 nm, MS (ESI) *m/z* = 434.1 [*M* + *H*]<sup>+</sup>.

**Protein expression and purification.** A codon-optimized gene sequence encoding residues 172-327 of human Mcl-1 (Uniprot: Q07820) was purchased (Genscript) and cloned into a Gateway entry vector (pDONR-221, Invitrogen) using the protocols provided. This construct was further sub-cloned into an expression vector (pDEST-HisMBP) containing a maltose binding protein (MBP) tag for increased solubility, a tobacco etch virus (TEV) protease recognition site for tag-removal and an N-terminal His-tag to facilitate purification. The integrity of all plasmids was checked by sequencing. Soluble Mcl-1 protein was expressed in *Escherichia coli* BL21 CodonPlus (DE3) RIL (Stratagene) using ampicillin and chloramphenicol for selection.

In brief, a colony from a fresh transformation plate was picked to inoculate 100 mL of LB medium (37°C). The overnight culture was used to start a 10 L fermentation (BioFlo 415, New Brunswick Scientific) grown at 37°C. For NMR studies, uniformly <sup>15</sup>N and <sup>15</sup>N/<sup>13</sup>C isotopically labeled protein samples were produced in minimal M9 media, where <sup>15</sup>NH<sub>4</sub>Cl and [U-<sup>13</sup>C]-D-glucose were used as sole nitrogen and carbon sources (Cambridge Isotope Laboratories). When the cell density corresponded to OD<sub>600</sub>=2, the temperature was lowered to 20°C. After one hour,

protein expression was induced with 0.5 mM IPTG. Cells were harvested after 16 h by centrifugation. Pellets were frozen and re-dissolved in lysis buffer (20 mM TRIS pH 7.5, 300 mM NaCl, 20 mM imidazole, 5 mM BME), approximately 100 mL / 10 g pellet, before the cells were broken by homogenization (APV-2000, APV). Prior to application to an affinity column (140 mL, ProBond, Invitrogen), lysate was cleared by centrifugation (18,000 rpm) and filtration (0.44  $\mu$ m). Bound protein was washed on the column and then eluted by a gradient (20 mM TRIS pH 7.5, 300 mM NaCl, 500 mM imidazole, 5 mM BME). To enhance TEV protease cleavage, samples were buffer exchanged (50 mM TRIS pH 7.5, 100 mM NaCl, 5 mM BME) on three serially connected columns (HiPrep 26/10 Desalting, GE Healthcare). TEV protease was added to a molar ratio of 1:10 (TEV:Mcl-1) and incubated at room temperature until cleavage was complete. After adding 20 mM imidazole to the samples, they were passed over a subtractive second nickel-column (120 mL, Ni-NTA Superflow, Qiagen) to remove the MBP-tag, non-cleaved protein, and TEV protease. Mcl-1 protein for NMR screening was buffer exchanged into an optimized NMR buffer (25 mM sodium phosphate pH 6.3, 25 mM NaCl, 1 mM DTT, 0.01%  $\text{NaN}_3$ ). To achieve highly pure samples (e.g. for crystal screening), a supplementary step of size-exclusion chromatography (HiLoad 26/60, Superdex 75, GE Healthcare) was implemented. The running buffer also acted as the Mcl-1 storage and crystallography buffer (20 mM HEPES pH 6.8, 50 mM NaCl, 3 mM DTT, 0.01%  $\text{NaN}_3$ ). Purifications were done at 4°C, and concentration steps were performed in stirred ultrafiltration cells (Amicon, Millipore).

To improve protein sample quality and to increase crystal diffraction, protein mutants were created by site-directed mutagenesis (QuikChange, Agilent Technologies). Primers for a C-terminal deletion ( $\Delta 5$ ) were designed using their online tool and ordered from Eurofins MWG

Operon. Mutations were made on the entry vector above, analyzed by in-house sequencing, and subsequently transferred into the pDEST-HisMBP expression vector. Mutant proteins were purified in the same way as wild-type (WT) proteins.

***NMR experiments NOE-guided fragment docking.*** NOE-derived distance restraints were acquired to enable NMR-based docking of fragments into a previously determined X-ray structure of a Mcl-1/ligand complex (PDB: 4HW2). Spectra were recorded on a Bruker 800-MHz spectrometer equipped with a cryo-probe and pulsed field gradients. 300  $\mu\text{M}$   $^{15}\text{N}/^{13}\text{C}$ -labeled samples of Mcl-1 was prepared in a  $\text{D}_2\text{O}$ -based NMR buffer and mixed with fragment **2** at a concentration of 1 mM. Side-chain  $^1\text{H}$  and  $^{13}\text{C}$  NMR signals were assigned from  $^{13}\text{C}$ -edited NOE and HCCH-TOCSY experiments.<sup>41,42</sup> NOE distance restraints were obtained from three-dimensional  $^{13}\text{C}$ -edited NOESY spectra, as well as three-dimensional  $^{15}\text{N}$ - and  $^{13}\text{C}$ -filter/edit NOESY spectra acquired with a mixing time of 80 ms. Compounds were docked into a X-ray structure using the NMR-derived restraints and a simulated annealing protocol using the program Xplor-NIH.<sup>43</sup> A square-well potential ( $F_{\text{NOE}} = 50 \text{ kcal mol}^{-1}$ ) was employed to constrain NOE-derived distances. Five low energy models from this process were energy minimized using MOE 2011.10 (Chemical Computing Group Inc., Montreal). The lowest energy structures obtained by this method were consistent with the observed NOEs.

***Protein crystallization, data collection and structure refinement.*** Fresh batches of Mcl-1 proteins, WT and  $\Delta 5$ , were concentrated to 600  $\mu\text{M}$  (10.7 mg/mL) and 1 mM (17.4 mg/mL), respectively, and screened for crystallization conditions with a 1.2x excess of ligand. Crystals were obtained by mixing 1  $\mu\text{L}$  protein with 1  $\mu\text{L}$  reservoir solution (25-30% PEG 3350, 0.1 M

Bis-TRIS pH 6.5, 0.2 M MgCl<sub>2</sub>) as a hanging drop at 4°C or 18°C. Crystals appeared within the first week and were flash frozen in liquid nitrogen after cryoprotection using 10-20% glycol.

Data were collected on the Life Sciences Collaborative Access Team (LS-CAT) 21-ID-D beamline at the Advanced Photon Source (APS), Argonne National Laboratory. Indexing, integration and scaling was performed with HKL2000.<sup>44</sup> Using a previously determined ligand-bound structure (PDB: 4HW2), phasing was done by molecular replacement with Phaser<sup>45</sup> as implemented in CCP4.<sup>46</sup> Refinement of the structural models were performed with Phenix<sup>47</sup> and Refmac<sup>48</sup>, and included rounds of manual model building in COOT.<sup>49</sup> Figures were prepared in PyMOL<sup>50</sup> and MOE.

**FPA Competition Assays.** A fluorescein isothiocyanate (FITC)-labeled BH3 peptide derived from Bak (FITC-Bak-BH3; FITC-AHx-GQVGRQLAIIGDDINR-NH<sub>2</sub>) was purchased from GenScript and used without further purification. FPA measurements were carried out in 384-well, black, flat-bottom plates (Greiner Bio-One) using the EnVision plate reader (PerkinElmer). All assays were conducted in assay buffer containing 20 mM TRIS pH 7.5, 50 mM NaCl, 3 mM DTT, and 5% final DMSO concentration. To measure displacement of the FITC-Bak-BH3 peptide from Bcl-2 family members, 10 nM FITC-Bak-BH3 peptide was incubated with either 15 nM Mcl-1 or 4 nM Bcl-xL. For IC<sub>50</sub> determination, compounds were diluted in DMSO in a 10-point, 3-fold serial dilution scheme, added to assay plates, and incubated for 1.5 h at room temperature. The change in anisotropy was measured and used to calculate an IC<sub>50</sub> (inhibitor concentration at which 50% of bound peptide is displaced) by fitting the anisotropy data using XLFit (IDBS) to a four parameter dose-response (variable slope) equation. This was converted into a binding dissociation constant (K<sub>i</sub>) according to the formula<sup>51</sup>:

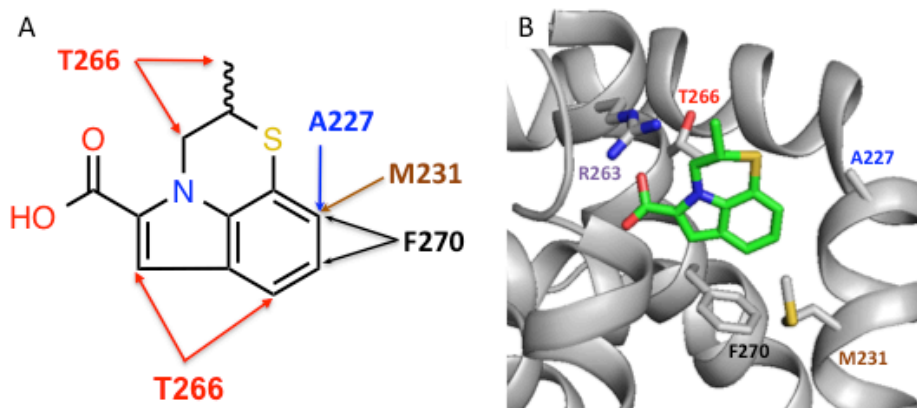
$$K_i = [I]_{50}/([L]_{50}/K_d + [P]_0/K_d + 1)$$

where  $[I]_{50}$  is the concentration of the free inhibitor at 50% inhibition,  $[L]_{50}$  is the concentration of the free labeled ligand at 50% inhibition,  $[P]_0$  is the concentration of the free protein at 0% inhibition and  $K_d$  represents the dissociation constant of the FITC-labeled peptide probe. Compounds were evaluated using replicate measurements, in duplicate;  $K_i$  values shown are the average of duplicate values.

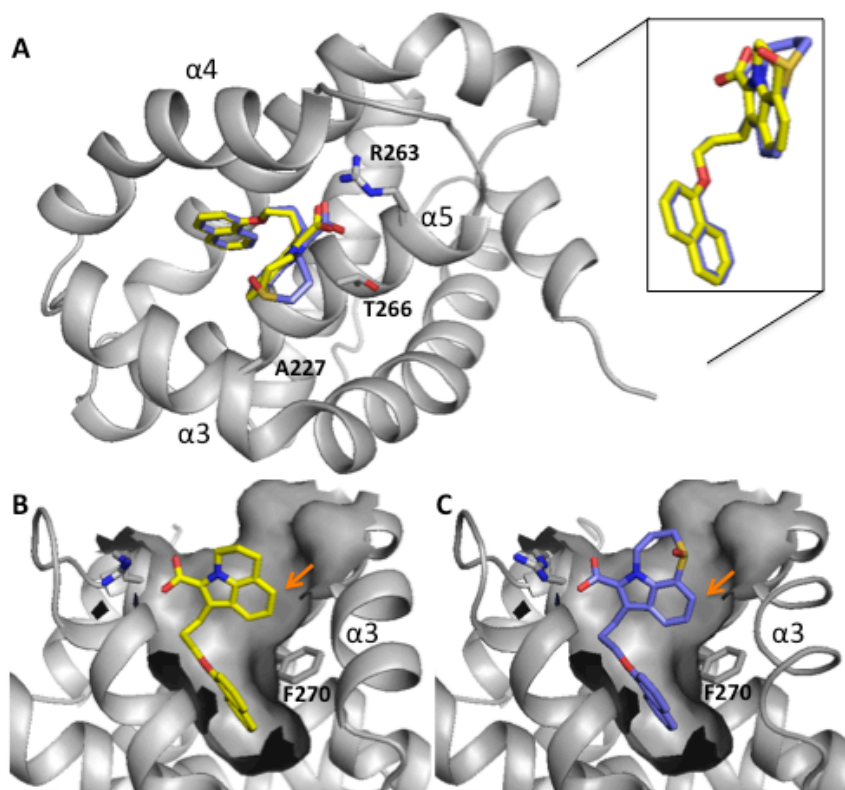
***Biotin streptavidin pull-down experiment.*** Human chronic myelogenous leukemia K562 cells were grown in RPMI-8226 complete media, lysed in NP-40 buffer (150mM NaCl, 1% NP-40, 50mM Tris, pH 8.0), cleared by centrifugation, and incubated with indicated concentrations of compound or Bim-BH3 peptide (FITC-Ahx-EARIAQELRRIGDEFNETYTR, Genscript) for 60 minutes at room temperature. Separately, Dynabeads M-280 streptavidin conjugated beads (Life Technologies) were incubated with biotin-Ahx-MS-1, an Mcl-1 specific peptide<sup>39</sup>, for 30 minutes and washed four times with PBS plus 0.01% TWEEN-20. The loaded beads were then incubated with lysate at room temperature for ten minutes, washed twice, boiled in SDS-PAGE loading buffer, and analyzed by Western blot (Licor Odyssey) with an Mcl-1 specific antibody (Y37, Abcam).



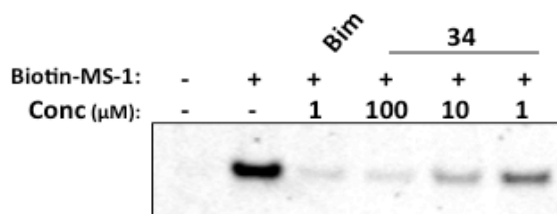
Figure 1



**Figure 1.** (A) Observed NOE interactions between Mcl-1 and compound **2**. (B) Model structures of Mcl-1 complexed to fragment hit **2** using NMR-derived distance restraints. Residues (labeled) with NOEs to fragment **2** (green) are rendered as sticks (gray). R263 is also labeled.

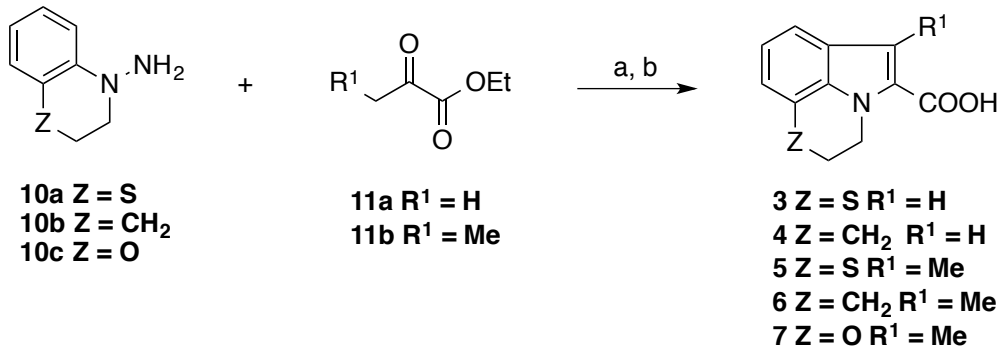
**Figure 2.**

**Figure 2.** X-ray structures of tricyclic indole acids bound to Mcl-1. (A) Compounds **17** and **24** interact with Mcl-1 in the BH3-peptide binding cleft between helices 3, 4, and 5. The indole cores and naphthyl groups adopt almost the same binding poses while C-ring units adopt different binding conformations (inset). Shown is the surface depiction of Mcl-1 when complexed to (B) Compound **17** and (C) Compound **24** that illustrates how these ligands occupy the P2 pocket. Arrows indicate potential positions for substitutions to fill unoccupied sub-sites.

**Figure 3.**

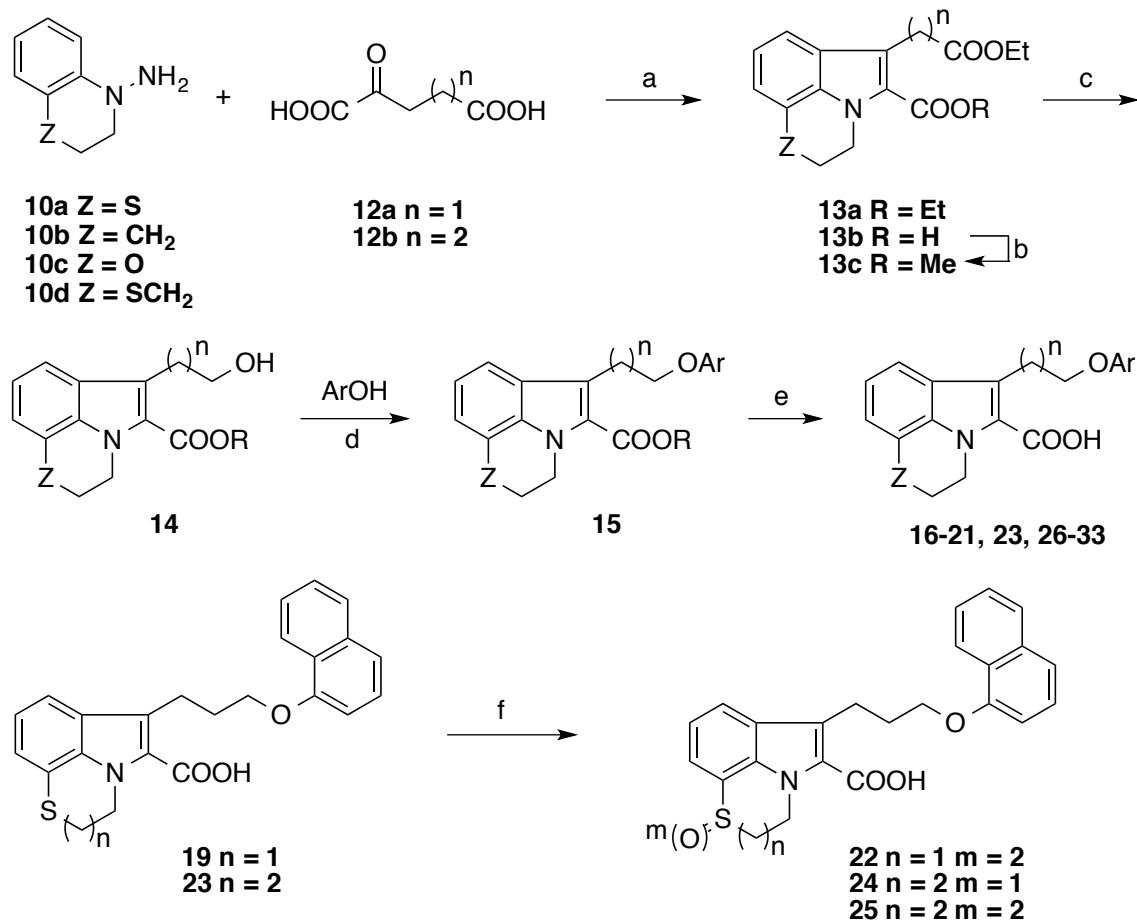
**Figure 3.** Compound 34 inhibits binding of biotin-MS-1 to Mcl-1 in cell lysates. K562 cell lysates were incubated with compound or a Bim-BH3 peptide positive control at indicated concentrations. Streptavidin-conjugated beads bound with biotin-MS-1 were incubated with the lysates to pulldown cellular Mcl-1, which was visualized by Western blot.

**Scheme 1. Synthesis of tricyclic indole carboxylic acid cores**



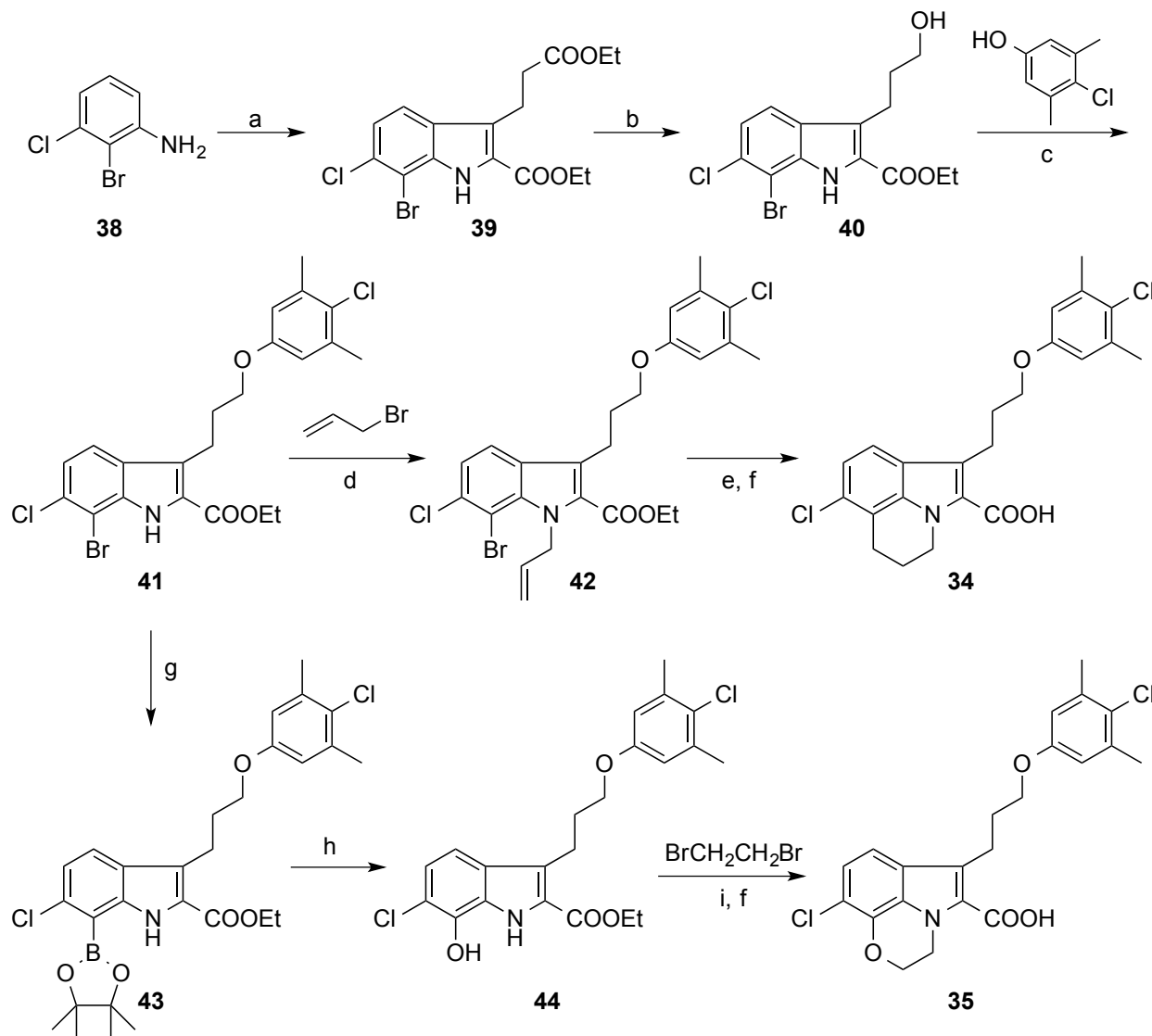
(a)  $EtOH, H_2SO_4$ ; (b)  $KOH (aq.), THF$ , 56-90% (two steps).

## Scheme 2. Synthesis of tricyclic indole carboxylic acid derivatives



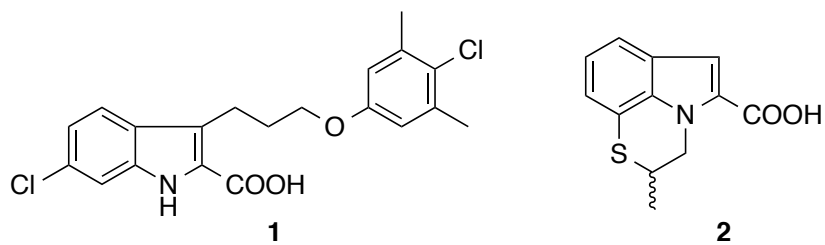
(a) EtOH, H<sub>2</sub>SO<sub>4</sub>; (b) TMSCHN<sub>2</sub> (2M in hexane), MeOH, benzene; (c) BH<sub>3</sub>-THF, THF; 20% (d) Dt-BuAD, PPh<sub>3</sub>, THF; (e) KOH (aq.), THF, 12-45% (six steps); (f) *m*-CPBA, CH<sub>2</sub>Cl<sub>2</sub>, 56-88%.

## Scheme 3. Synthesis of tricyclic 6-Cl-2-indole carboxylic acid derivatives



(a) (1)  $\text{NaNO}_2$ ,  $\text{HCl}$ , sodium acetate, ethyl 2-oxocyclopentane carboxylate,  $\text{H}_2\text{O}$ , 60% (two steps); (2)  $\text{EtOH}$ ,  $\text{H}_2\text{SO}_4$ ; (b)  $\text{BH}_3$ -THF, THF, 83%; (c) Dt-BuAD,  $\text{PPh}_3$ , THF, 82%; (d)  $\text{Cs}_2\text{CO}_3$ , DMF, 95%; (e) AIBN,  $\text{Bu}_3\text{SnH}$ , toluene; (f)  $\text{LiOH}$  (aq.), THF, 50% (two steps); (g) bis(pinacolato)diboron,  $\text{Pd}(\text{dppf})_2\text{Cl}_2 \cdot \text{CH}_2\text{Cl}_2$ , DMF, 35%; (h)  $\text{H}_2\text{O}_2$ ,  $\text{NaOH}$  (aq.), THF, 28%; (i)  $\text{Cs}_2\text{CO}_3$ , DMF, 74%.

Structure of Compound 1 & 2.



Structure of Compound 36 & 37.

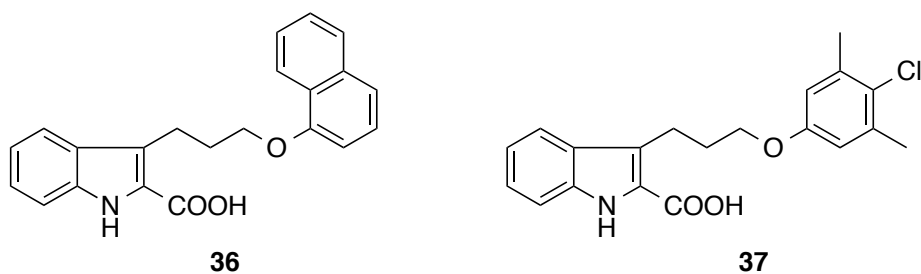
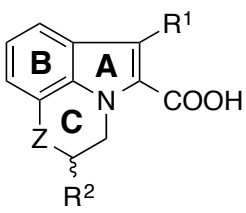


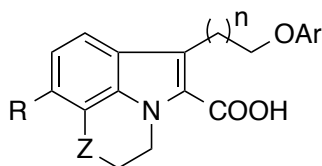
Table 1. SAR of tricyclic indole 2-carboxylic acids for binding to Mcl-1.



compd	Z	R <sup>1</sup>	R <sup>2</sup>	K <sub>i</sub> (μM)	LE
2	S	H	Me	35	0.38
3	S	H	H	51	0.39
4	CH <sub>2</sub>	H	H	131	0.35
5	S	Me	H	18	0.41
6	CH <sub>2</sub>	Me	H	90	0.35
7	O	Me	H	18	0.41
8	2-Indole-COOH			>1000	



Table 2. SAR of the merged tricyclic indole derivatives for binding to Mcl-1 and Bcl-xL



compd	Z	n	R	Ar	$K_i$ ( $\mu$ M)		
					Mcl-1	Bcl-xL	Bcl-2
<b>16</b>	S	1	H	1-naphthyl	3.0	9.0	
<b>17</b>	CH <sub>2</sub>	1	H	1-naphthyl	4.0	>20	
<b>18</b>	O	1	H	1-naphthyl	1.6	12.7	
<b>19</b>	S	2	H	1-naphthyl	0.12	>20	3.1
<b>20</b>	CH <sub>2</sub>	2	H	1-naphthyl	0.31	>20	7.3
<b>21</b>	O	2	H	1-naphthyl	0.11	1.9	5.7
<b>22</b>	SO <sub>2</sub>	2	H	1-naphthyl	0.088	>20	
<b>23</b>	SCH <sub>2</sub>	2	H	1-naphthyl	0.17	7.4	9.9
<b>24</b>	SOCH <sub>2</sub>	2	H	1-naphthyl	0.074	>20	16.0
<b>25</b>	SO <sub>2</sub> CH <sub>2</sub>	2	H	1-naphthyl	0.061	>20	11.7
<b>26</b>	S	2	H	1-(5,6,7,8-tetrahydronaphthyl)	0.150	3.0	3.7
<b>27</b>	S	2	H	1-(4-Cl-naphthyl)	0.200	4.7	1.1
<b>28</b>	S	2	H	2-(5,6,7,8-tetrahydronaphthyl)	0.410	>20	4.4
<b>29</b>	S	2	H	3-Me-4-Cl-phenyl	0.210	>20	6.3
<b>30</b>	S	2	H	3,5-di-Me-4-Cl-phenyl	0.071	>20	2.3
<b>31</b>	CH <sub>2</sub>	2	H	3,5-di-Me-4-Cl-phenyl	0.110	7.8	
<b>32</b>	O	2	H	3,5-di-Me-4-Cl-phenyl	0.065		
<b>33</b>	SCH <sub>2</sub>	2	H	3,5-di-Me-4-Cl-phenyl	0.040	>20	3.7
<b>34</b>	CH <sub>2</sub>	2	Cl	3,5-di-Me-4-Cl-phenyl	0.003	5.2	0.77
<b>35</b>	O	2	Cl	3,5-di-Me-4-Cl-phenyl	0.009	>20	1.3

## ASSOCIATED CONTENT

PDB ID codes: XXXX (*in process*)

## AUTHOR INFORMATION

### Corresponding Author

\*Phone: +1 (615) 322 6303. Fax: +1 (615) 875 3236. E-mail:stephen.fesik@vanderbilt.edu.

### Present Addresses

+ Currently at Institute for Applied Cancer Science, MD Anderson Cancer Center, 1901 East Road, Houston, TX 77054, USA

# Currently at Genzyme Corporation, 500 Kendall Street, Cambridge, MA 02142, USA

^ Currently at Bayer Healthcare, Berlin, Germany

### Funding Sources

Any funds used to support the research of the manuscript should be placed here (per journal style).

### Notes

The authors declare no competing financial interest.

## ACKNOWLEDGMENT

The authors thank co-workers at the High-Throughput Screening Core facility of Vanderbilt University, TN, for compound management and providing the instrumentation to perform the binding assay. This research was supported by the U.S. National Institutes of Health, NIH

Director's Pioneer Award DP1OD006933/DP1CA174419 to S.W.F., The NCI Experimental Therapeutics (NExT) Program BOA29XS129TO22 under the Leidos Biomed Prime Contract No. HHSN261200800001E, and a career development award to S.W.F. from a NCI SPORE grant in breast cancer (Grant P50CA098131) to C. L. Arteaga. This work was also funded by the American Cancer Society (Postdoctoral Fellowship, Grant PF1110501CDD) to J.P.B. The Biomolecular NMR Facility at Vanderbilt University is supported in part by a NIH SIG Grant 1S-10RR025677-01 and Vanderbilt University matching funds. Use of the Advanced Photon Source was supported by the U.S. Department of Energy, Office of Science, Office of Basic Energy Sciences, under Contract No. DE-AC02-06CH11357.

## ABBREVIATIONS

Mcl-1, myeloid cell leukemia 1; Bcl-2, B-cell lymphoma 2; Bcl-xL, B-cell lymphoma extra large; BH3, Bcl-2 homology domain 3; Bax, Bcl-2-associated X protein; Bak, Bcl-2 homologous antagonist killer; LE, ligand efficiency; *m*-CPBA, meta-chloroperoxybenzoic acid; NOE, Nuclear Overhauser Effect; FITC, fluorescein isothiocyanate; FPA, fluorescence polarization anisotropy.

---

## REFERENCES

- (1) Danial, N. N.; Korsmeyer, S. J. Cell Death: Critical Control Points. *Cell* **2004**, *116*, 205-219.
- (2) Kroemer, G.; Galluzzi, L.; Brenner, C. Mitochondrial Membrane Permeabilization in Cell Death. *Physiol. Rev.*, **2007**, *87*, 99-163.
- (3) Cory, S.; Adams, J. M. The Bcl2 Family: Regulators of the Cellular Life-or-Death Switch. *Nat. Rev. Cancer* **2002**, *2*, 647-656.
- (4) Adams, J. M.; Cory, S. The Bcl-2 Apoptotic Switch in Cancer Development and Therapy. *Oncogene* **2007**, *26*, 1324-1337.
- (5) Wei, G.; Margolin, A. A.; Haery, L.; Brown, E.; Cucolo, L.; Julian, B.; Shehata, S.; Kung, A. L.; Beroukhi, R.; Golub, T. R. Chemical Genomics Identifies Small-Molecule MCL1 Repressors and BCL-xL as a Predictor of MCL1 Dependency. *Cancer Cell* **2012**, *21*, 547-562.
- (6) Beroukhi, R.; Mermel, C. H.; Porter, D.; Wei, G.; Raychaudhuri, S.; Donovan, J.; Barretina, J.; Boehm, J. S.; Dobson, J.; Urashima, M.; McHenry, K. T.; Pinchback, R. M.; Ligon, A. H.; Cho, Y.-J.; Haery, L.; Greulich, H.; Reich, M.; Winckler, W.; Lawrence, M. S.; Weir, B. A.; Tanaka, K. E.; Chiang, D. Y.; Bass, A. J.; Loo, A.; Hoffman, C.; Prensner, J.; Liefeld, T.; Gao, Q.; Yecies, D.; Signoretti, S.; Maher, E.; Kaye, F. J.; Sasaki, H.; Tepper, J. E.; Fletcher, J. A.; Tabernero, J.; Baselga, J.; Tsao, M.-S.; Demichelis, F.; Rubin, M. A.; Janne, P. A.; Daly, M. J.; Nucera, C.; Levine, R. L.; Ebert, B. L.; Gabriel, S.; Rustgi, A. K.; Antonescu, C. R.; Ladanyi, M.; Letai, A.; Garraway, L. A.; Loda, M.; Beer, D. G.; True, L. D.; Okamoto, A.; Pomeroy, S. L.; Singer, S.; Golub, T. R.; Lander, E. S.; Getz, G.; Sellers, W. R.; Meyerson, M. The Landscape of Somatic Copy-Number Alteration Across Human Cancers. *Nature* **2010**, *463*, 899-905

- 
- (7) Song, L.; Coppola, D.; Livingston, S.; Cress, D.; Haura, E. B. Mcl-1 Regulates Survival and Sensitivity to Diverse Apoptotic Stimuli in Human Non-Small Cell Lung Cancer Cells. *Cancer Biol. Ther.* **2005**, *4*, 267-276.
- (8) Ding, Q.; He, X.; Xia, W.; Hsu, J.-M.; Chen, C.-T.; Li, L.-Y.; Lee, D.-F.; Yang, J.-Y.; Xie, X.; Liu, J.-C.; Hung, M.-C. Myeloid Cell Leukemia-1 Inversely Correlates with Glycogen Synthase Kinase-3 $\beta$  Activity and Associates with Poor Prognosis in Human Breast Cancer. *Cancer Res.* **2007**, *67*, 4564-4571.
- (9) Krajewska, M.; Krajewski, S.; Epstein, J. I.; Shabaik, A.; Sauvageot, J.; Song, K.; Kitada, S.; Reed, J. C. Immunohistochemical Analysis of Bcl-2, Bax, Bcl-X, and Mcl-1 Expression in Prostate Cancers. *Am. J. Pathol.* **1996**, *148*, 1567-1576.
- (10) Miyamoto, Y.; Hosotani, R.; Wada, M.; Lee, J. U.; Koshiba, T.; Fujimoto, K.; Tsuji, S.; Nakajima, S.; Doi, R.; Kato, M.; Shimada, Y.; Imamura, M. Immunohistochemical Analysis of Bcl-2, Bax, Bcl-X, and Mcl-1 Expression in Pancreatic Cancers. *Oncology* **1999**, *56*, 73-82.
- (11) Brotin, E.; Meryet-Figuiere, M.; Simonin, K.; Duval, R. E.; Villedieu, M.; Leroy-Dudal, J.; Saison-Behmoaras, E.; Gauduchon, P.; Denoyelle, C.; Poulain, L. Bcl-XL and MCL-1 Constitute Pertinent Targets in Ovarian Carcinoma and Their Concomitant Inhibition Is Sufficient to Induce Apoptosis. *Int. J. Cancer* **2010**, *126*, 885-895.
- (12) Zhang, T.; Zhao, C.; Luo, L.; Zhao, H.; Cheng, J.; Xu, F. The Expression of Mcl-1 in Human Cervical Cancer and Its Clinical Significance. *Med. Oncol.* **2012**, *29*, 1985-91.
- (13) Derenne, S.; Monia, B.; Dean, N. M.; Taylor, J. K.; Rapp, M.-J.; Harousseau, J.-L.; Bataille, R.; Amiot, M. Antisense Strategy Shows that Mcl-1 Rather than Bcl-2 or Bcl-xL Is an Essential Survival Protein of Human Myeloma Cells. *Blood* **2002**, *100*, 194-199.
- (14) Andersen, M. H.; Becker, J. C.; Thor Straten, P. The Antiapoptotic Member of the Bcl-2

family Mcl-1 Is a CTL Target in Cancer Patients. *Leukemia* **2005**, *19*, 484-485.

(15) Wertz, I. E.; Kusam, S.; Lam, C.; Okamoto, T.; Sandoval, W.; Anderson, D. J.; Helgason, E.; Ernst, J. A.; Eby, M.; Liu, J.; Belmont, L. D.; Kaminker, J. S.; O'Rourke, K. M.; Pujara, K.; Kohli, P. B.; Johnson, A. R.; Chiu, M. L.; Lill, J. R.; Jackson, P. K.; Fairbrother, W. J.; Seshagiri, S.; Ludlam, M. J. C.; Leong, K. G.; Dueber, E. C.; Maecker, H.; Huang, D. C. S.; Dixit, V. M. Sensitivity to Antitubulin Chemotherapeutics Is Regulated by MCL1 and FBW7. *Nature* **2011**, *471*, 110-114.

(16) Arkin, M.R. & Wells, J.A. Small-Molecule Inhibitors of Protein-Protein Interactions: Progressing Towards the Dream. *Nat. Rev. Drug Discov.* **2004**, *3*, 301-317.

(17) Lessene, G.; Czabotar, P. E.; Colman, P. M. BCL-2 family antagonists for cancer therapy. *Nat. Rev. Drug Discovery* **2008**, *7*, 989-1000.

(18) Lessene, G.; Czabotar, P.E.; Sleebs, B.E.; Zobel K.; Lowes, K.N.; Adams, J.M.; Baell, J.B.; Colman, P.M.; Deshayes, K.; Fairbrother, W.J.; Flygare, J.A.; Gibbons, P.; Kersten, W.J.; Kulasegaram, S.; Moss, R.M.; Parisot, J.P.; Smith, B.J.; Street, I.P.; Yang, H.; Huang, D.C.; Watson, K.G. Structure-guided design of a selective BCL-X(L) inhibitor. *Nat. Chem. Biol.* **2013**, *9*, 390-397.

(19) Wendt, M. D.; Wang Shen, W.; Kunzer, A.; McClellan, W. J.; Bruncko, M.; Oost, T. K.; Ding, H.; Joseph, M. K.; Zhang, H.; Nimmer, P. M.; Ng, S.-H.; Shoemaker, A. R.; Petros, A. M.; Oleksijew, A.; Marsh, K.; Bauch, J.; Oltersdorf, T.; Belli, B. A.; Martineau, D.; Fesik, S. W.; Rosenberg, S. H.; Elmore, S. W. Discovery and Structure-Activity Relationship of Antagonists of B-Cell Lymphoma 2 Family Proteins with Chemopotential Activity in Vitro and in Vivo. *J. Med. Chem.* **2006**, *49*, 1165-1181.

- (20) Bruncko, M.; Oost, T. K.; Belli, B. A.; Ding, H.; Joseph, M. K.; Kunzer, A.; Martineau, D.; McClellan, W. J.; Mitten, M.; Ng, S.-C.; Nimmer, P. M.; Oltersdorf, T.; Park, C.-M.; Petros, A. M.; Shoemaker, A. R.; Song, X.; Wang, X.; Wendt, M. D.; Zhang, H.; Fesik, S. W.; Rosenberg, S. H.; Elmore, S. W. Studies Leading to Potent, Dual Inhibitors of Bcl-2 and Bcl-xL. *J. Med. Chem.* **2007**, *50*, 641-662.
- (21) Park, C.-M.; Bruncko, M.; Adickes, J.; Bauch, J.; Ding, H.; Kunzer, A.; Marsh, K. C.; Nimmer, P.; Shoemaker, A. R.; Song, X.; Tahir, S. K.; Tse, C.; Wang, X.; Wendt, M. D.; Yang, X.; Zhang, H.; Fesik, S. W.; Rosenberg, S. H.; Elmore, S. W. Discovery of an Orally Bioavailable Small Molecule Inhibitor of Prosurvival B-Cell Lymphoma 2 Protein. *J. Med. Chem.* **2008**, *51*, 6902-6915.
- (22) Petros, A. M.; Huth, J. R.; Oost, T.; Park, C.-M.; Ding, H.; Wang, X.; Zhang, H.; Nimmer, P.; Mendoza, R.; Sun, C.; Mack, J.; Walter, K.; Dorwin, S.; Gramling, E.; Lador, U.; Rosenberg, S. H.; Elmore, S. W.; Fesik, S. W.; Hajduk, P. J. Discovery of a Potent and Selective Bcl-2 Inhibitor Using SAR by NMR. *Bioorg. Med. Chem. Lett.* **2010**, *20*, 6587-6591.
- (23) Zhou, H.; Chen, J.; Meagher, J. L.; Yang, C.-Y.; Aguilar, A.; Liu, L.; Bai, L.; Cong, X.; Cai, Q.; Fang, X.; Stuckey, J. A.; Wang, S. Design of Bcl-2 and Bcl-xL Inhibitors with Subnanomolar Binding Affinities Based upon a New Scaffold. *J. Med. Chem.* **2012**, *55*, 4664-4682.
- (24) Souers, A. J.; Levenson, J. D.; Boghaert, E. R.; Ackler, S. L.; Catron, N. D.; Chen, J.; Dayton, B. D.; Ding, H.; Enschede, S. H.; Fairbrother, W. J.; Huang, C. C. S.; Hymowitz, S. G.; Jin, S.; Khaw, S. L.; Kovar, P. J.; Lam, L. T.; Lee, J.; Maecker, H. L.; Marsh, K. C.; Mason, K. D.; Mitten, M. J.; Nimmer, P. M.; Oleksijew, A.; Park, C. H.; Park, C.-M.; Phillips, D. C.; Roberts, A. W.; Sampath, D.; Seymour, J. F.; Smith, M. L.; Sullivan, G. M.; Tahir, S. K.; Tse, C.; Wendt, M. D.; Xiao, Y.; Xue, J. C.; Zhang, H.; Humerickhouse, R. A.; Rosenberg, S. H.;

Elmore, S. W. ABT-199, a Potent and Selective BCL-2 Inhibitor, Achieves Antitumor Activity While Sparing Platelets. *Nature Medicine* **2013**, *19*, 202-210.

(25) Tao, Z.-F.; Hasvold, L.; Wang, L.; Wang, X.; Petros, A. M.; Park, C. H.; Boghaert, E. R.; Catron, N. D.; Chen, J.; Colman, P. M.; Czabotar, P. E.; Deshayes, K.; Fairbrother, W. J.; Flygare, J. A.; Hymowitz, S. G.; Jin, S.; Judge, R. A.; Koehler, M. F. T.; Kovar, P. J.; Lessene, G.; Mitten, M. J.; Ndubaku, C. O.; Nimmer, P.; Purkey, H. E.; Oleksijew, A.; Phillips, D. C.; Sleebs, B. E.; Smith, B. J.; Smith, M. L.; Tahir, S. K.; Watson, K. G.; Xiao, Y.; Xue, J.; Zhang, H.; Zobel, K.; Rosenberg, S. H.; Tse, C.; Levenson, J. D.; Elmore, S. W.; Souers, A. J. Discovery of a Potent and Selective BCL<sub>2</sub>XL Inhibitor with *in Vivo* Activity. *ACS Med. Chem. Lett.* **2014**, *5*, 1088-1093.

(26) Wilson, W. H.; O'Connor, O. A.; Czuczman, M. S.; LaCasce, A. S.; Gerecitano, J. F.; Leonard, J. P.; Tulpule, A.; Dunleavy, K.; Xiong, H.; Chiu, Y. L.; Cui, Y.; Busman, T.; Elmore, S. W.; Rosenberg, S. H.; Krivoshik, A. P.; Enschede, S. H.; Humerickhouse, R. Navitoclax, a Targeted High-Affinity Inhibitor of BCL-2, in Lymphoid Malignancies: a Phase 1 Dose-Escalation Study of Safety, Pharmacokinetics, Pharmacodynamics, and Antitumour Activity. *Lancet Oncol.* **2010**, *11*, 1149-1159.

(27) Roberts, A. W.; Seymour, J. F.; Brown, J. R.; Wierda, W. G.; Kipps, T. J.; Khaw, S. L.; Carney, D. A.; He, S. Z.; Huang, D. C. S.; Xiong, H.; Cui, Y.; Busman, T. A.; McKeegan, E. M.; Krivoshik, A. P.; Enschede, S. H.; Humerickhouse, R. Substantial Susceptibility of Chronic Lymphocytic Leukemia to BCL2 Inhibition: Results of a Phase I Study of Navitoclax in Patients with Relapsed or Refractory Disease. *J. Clin. Oncol.* **2012**, *30*, 488-496.



- (28) Friberg, A.; Vigil, D.; Zhao, B.; Daniels, R. N.; Burke, J. P.; Garcia-Barrantes, P. M.; Camper, D.; Chauder, B. A.; Lee, T.; Olejniczak, E. T.; Fesik, S. W. Discovery of Potent Myeloid Cell Leukemia 1 (Mcl-1) Inhibitors Using Fragment-Based Methods and Structure-Based Design. *J. Med. Chem.* **2013**, *56*, 15-30.
- (29) Abulwerdi, F. A.; Liao, C.; Mady, A.; Gavin, J.; Shen, C.; Cierpicki, T.; Stuckey, J. A.; Showalter, H. D. H.; Nikolovska-Coleska, Z. 3-Substituted-N-(4-Hydroxynaphthalen-1-yl)arylsulfonamides as a Novel Class of Selective Mcl-1 Inhibitors: Structure-Based Design, Synthesis, SAR and Biological Evaluation. *J. Med. Chem.* **2014**, *57*, 4111-4133.
- (30) Zhang, Z.; Li, X.; Song, T.; Zhao, Y.; Feng, Y.; An Anthraquinone Scaffold for Putative, Two-Face Bim BH3  $\alpha$ -Helix Mimic. *J. Med. Chem.* **2012**, *55*, 10735-10741.
- (31) Petros, A. M.; Swann, S. L.; Song, D.; Swinger, K.; Park, C.; Zhang, H.; Wendt, M. D.; Kunzer, A. R.; Souers, A. J.; Sun, C. Fragment-Based Discovery of Potent Inhibitors of the Anti-Apoptotic MCL-1 Protein. *Bioorg. Med. Chem. Lett.* **2014**, *24*, 1484-1488.
- (32) Rega, M. F.; Wu, B.; Wei, J.; Zhang, Z.; Cellitti, J. F.; Pellecchia, M. SAR by Interligand Nuclear Overhauser Effects (ILOEs) Based Discovery of Acylsulfonamide Compounds Active against Bcl-xL and Mcl-1. *J. Med. Chem.* **2011**, *54*, 6000-6013.
- (33) Bian, Z.; Marvin, C.; Pettersson, M.; Martin, S. F. Enantioselective Total Syntheses of Citrinadins A and B. Stereochemical Revision of their Assigned Structures. *J. Am. Chem. Soc.* **2014**, *136*, 14184-14192.
- (34) Bian, Z.; Marvin, C.; Martin, S. F. Enantioselective Total Synthesis of (-)-Citrinadin A and Revision of its Stereochemical Structure. *J. Am. Chem. Soc.* **2013**, *135*, 10886-10889.
- (35) Caron, G.; Gaillard, P.; Carrupt, P.-A.; Testa, B. Lipophilicity Behavior of Model and

Medicinal Compounds Containing a Sulfide, Sulfoxide, or Sulfone Moiety. *Helv. Chim. Acta* **1997**, *80*, 449-462.

(36) Zhang, H.; Nimmer, P. M.; Tahir, S. K.; Chen, J.; Fryer, R. M.; Hahn, K. R.; Iciek, L. A.; Morgan, S. J.; Nasarre, M. C.; Nelson, R.; Preusser, L. C.; Reinhart, G. A.; Smith, M. L.; Rosenberg, S. H.; Elmore, S. W.; Tse, C. Bcl-2 family proteins are essential for platelet survival. *Cell Death Differ.* **2007**, *14*, 943–951.

(37) Mason, K. D.; Carpinelli, M. R.; Fletcher, J. I.; Collinge, J. E.; Hilton, A. A.; Ellis, S.; Kelly, P. N.; Ekert, P. G.; Metcalf, D.; Roberts, A. W.; Huang, D. C. S.; Kile, B. T. Programmed Anuclear Cell Death Delimits Platelet Life Span. *Cell* **2007**, *128*, 1173-1186.

(38) Abulwerdi, F.A.; Liao, C.; Mady, A.S.; Gavin, J.; Shen, C.; Cierpicki, T.; Stuckey J.A.; Showalter, H.D.; Nikolovska-Coleska, Z. 3-Substituted-N-(4-hydroxynaphthalen-1-yl)arylsulfonamides as a novel class of selective Mcl-1 inhibitors: structure-based design, synthesis, SAR, and biological evaluation. *J. Med. Chem.* **2014**, *57*, 4111-4133.

(39) Foight, G. W.; Ryan, J. A.; Gulla, S. V.; Letai, A.; Keating, A. E. Designed BH3 Peptides with High Affinity and Specificity for Targeting Mcl-1 in Cells. *ACS Chem. Bio.* **2014**, *9*, 1962-1968.

(40) Levenson, J.D. ; Zhang, H.; Chen, J. ; Tahir, S. K.; Phillips, D C.; Xue, J .; Nimmer<sup>1</sup>, S Jin, P.; Smith, M.; Xiao, Y.; Kovar, P.; Tanaka, A.; Bruncko, M.; Sheppard, G S.; Wang, L .; Gierke, S.; Kategaya, L.; Anderson, D J.; Wong, C .; Eastham-Anderson, J.; Ludlam, M J C.; Sampath, D.; Fairbrother, W J.; Wertz I .; Rosenberg, S H.; Tse, C.; Elmore S W. and Souers A. J. Potent and selective small-molecule MCL-1 inhibitors demonstrate on-target cancer cell killing activity

as single agents and in combination with ABT-263 (navitoclax). *Cell Death & Disease* **2015**, *6*, e1590

(41) Clore, G. M.; Gronenborn, A. M. *Methods Enzymol* **1994**, *239*, 349-363

(42) Sattler, M.; Schleucher, J.; Griesinger, C. Heteronuclear multidimensional NMR experiments for the structure determination of proteins in solution employing pulsed. *Prog. Nucl. Magn. Reson. Spectrosc.* **1999**, *34*, 93-158.

(43) Schwieters, C. D.; Kuszewski, J. J.; Tjandra, N.; Clore, G. M. The Xplor-NIH NMR molecular structure determination package. *J. Magn. Reson.* **2003**, *160*, 65-73.

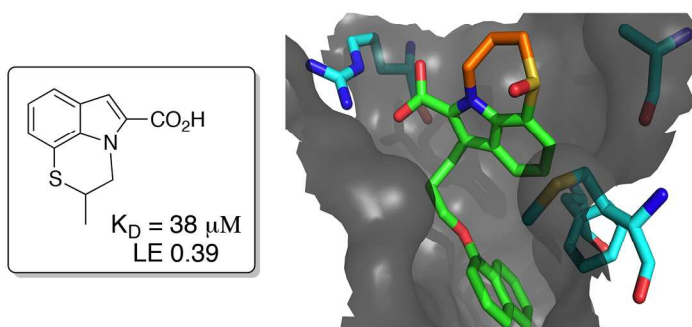
(44) Otwinowski, Z.; Minor, W. Processing of X-ray Diffraction Data Collected in Oscillation Mode. In *Macromolecular Crystallography. Part A*; Carter, C. W., Jr., Sweet, R. M., Eds.; Academic Press: San Diego, CA, 1997; Vol. 276, pp 307-326.

(45) McCoy, A. J.; Grosse-Kunstleve, R. W.; Adams, P. D.; Winn, M. D.; Storoni, L. C.; Read, R. J. Phaser crystallographic software. *J. Appl. Crystallogr.* **2007**, *40*, 658-674.

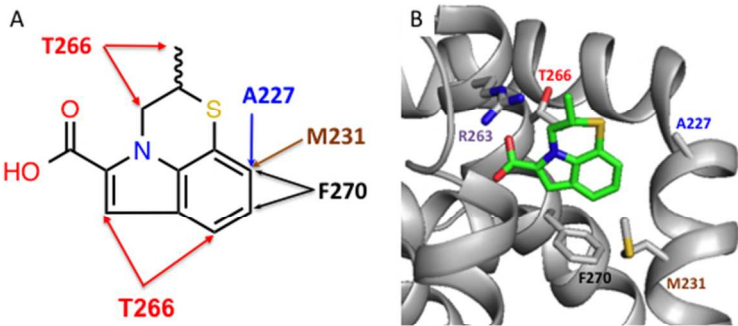
(46) Winn, M. D.; Ballard, C. C.; Cowtan, K. D.; Dodson, E. J.; Emsley, P.; Evans, P. R.; Keegan, R. M.; Krissinel, E. B.; Leslie, A. G. W.; McCoy, A.; McNicholas, S. J.; Murshudov, G. N.; Pannu, N. S.; Potterton, E. A.; Powell, H. R.; Read, R. J.; Vagin, A.; Wilson, K. S. Overview of the CCP4 suite and current developments. *Acta Crystallogr., Sect. D: Biol. Crystallogr.* **2011**, *67*, 235-242.

(47) Adams, P. D.; Grosse-Kunstleve, R. W.; Hung, L. W.; Ioerger, T. R.; McCoy, A. J.; Moriarty, N. W.; Read, R. J.; Sacchettini, J. C.; Sauter, N. K.; Terwilliger, T. C. PHENIX: building new software for automated crystallographic structure determination. *Acta Crystallogr., Sect. D: Biol. Crystallogr.* **2002**, *58*, 1948-1954.

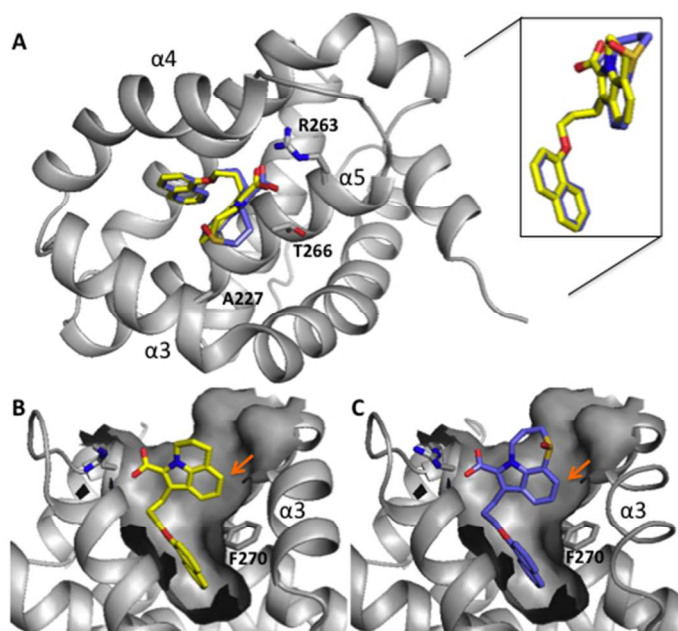
- 
- (48) Murshudov, G. N.; Skubák, P.; Lebedev, A. A.; Pannu, N. S.; Steiner, R. A.; Nicholls, R. A.; Winn, M. D.; Long, F.; Vagin, A. A. REFMAC5 for the refinement of macromolecular crystal structures. *Acta Crystallogr., Sect. D: Biol. Crystallogr.* **2011**, *67*, 355–367.
- (49) Emsley, P.; Cowtan, K. Coot: model-building tools for molecular graphics. *Acta Crystallogr., Sect. D: Biol. Crystallogr.* **2004**, *60*, 2126–2132.
- (50) *The PyMOL Molecular Graphics System*, version 1.5; Schrödinger, LLC: New York, 2010.
- (51) Wang, Z. X.; Jiang, R. F. A novel two-site binding equation presented in terms of the total ligand concentration. *FEBS Lett.* **1996**, *392*, 245–249.



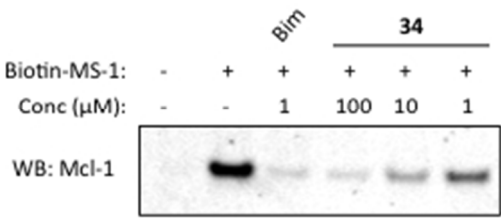
152x203mm (300 x 300 DPI)



254x190mm (72 x 72 DPI)



254x190mm (72 x 72 DPI)



99x49mm (72 x 72 DPI)